

1  
2  
3  
4  
5  
6  
7  
8  
9  
10  
11  
12  
13  
14  
15  
16  
17  
18  
19  
20  
21  
22  
23  
24  
25  
26  
27  
28  
29  
30  
31  
32  
33  
34  
35  
36  
37  
38  
39  
40  
41  
42  
43  
44  
45  
46  
47  
48  
49  
50  
51  
52  
53  
54  
55  
56  
57  
58  
59  
60  
61  
62  
63  
64  
65

## Attenuation processes of solar radiation. Application to the quantification of direct and diffuse solar irradiances on horizontal surfaces in Mexico by means of an overall atmospheric transmittance

Antonio J. Gutiérrez-Trashorras<sup>a,\*</sup>, Eunice Villicaña-Ortiz<sup>b</sup>, Eduardo Álvarez-Álvarez<sup>a</sup>, Juan M. González-Caballín<sup>a</sup>, Jorge Xiberta-Bernat<sup>a</sup> María José Suarez-López<sup>a</sup>

<sup>a</sup> Departamento de Energía, Escuela Técnica Superior de Ingenieros de Minas, Universidad de Oviedo, C/ Independencia, 13, 2<sup>a</sup> Planta, 33004 Oviedo, Spain

<sup>b</sup> Departamento de Ingeniería de la Energía. Universidad de Ingeniería y Tecnología. Lima, Perú.  
(Formerly: Departamento de Energías Renovables. Universidad Tecnológica del Centro de Veracruz. Mexico)

### List of acronyms

ANN	Artificial Neural Network
GIS	Geographic Information System
NASA	National Aeronautics and Space Administration
OAT	Overall atmospheric transmittance
RMSE	Root Mean Square Error

### Measurement units

Å	angstrom
µm	micrometer
masl	meters above sea level
W/m <sup>2</sup>	watt per square meter

## Abstract

Quantifying incident solar radiation on a surface is a complex task that requires the knowledge of geometric, geographical, astronomical, physical and meteorological characteristics of the location. The aim of this paper is to analyze the attenuation processes of the solar radiation and to review the scientific works in this field, specifically the analytical models for solar irradiance calculation, as well as to establish an alternative method to compute the magnitude of the overall atmospheric transmittance. Analytical models have been developed since 1940 and they have been improving in precision and complexity. Up until now, the Bird & Hulstrom model is the most complete and accurate of them all. The main disadvantage of this model is that a great number of equations and parameters such as temperature, sunshine hours, humidity, etc. are required.

In this paper, a very fast and accurate new method is developed to quantify solar irradiances at any site. The analysis shows that the parameters required are only the type of climate, altitude and state of the atmosphere. This method also allows to quantify the influence of the turbidity degree in both direct and diffuse irradiances. That information is essential to select which solar technologies are suitable in each place.

As an application, the new method has been implemented and characterized in Mexico. Solar energy is an abundant resource in Mexico, and there are some studies about the solar energy potential in that country, but the influence of physical and meteorological factors on the solar radiation have not been related. In this study, the meteorological information of 74 weather stations located in different climates of the country were used to determine the parameters required. The results have been validated with experimental data available for different locations.

**Keywords:** analytical models, scattering and absorption, direct and diffuse, atmospheric and climate parameters, solar radiation, renewable energy, sustainable energy

---

\*Corresponding author. Departamento de Energía, Escuela Técnica Superior de Ingenieros de Minas, Universidad de Oviedo, C/ Independencia, 13, 2<sup>a</sup> Planta, 33004 Oviedo, Spain. Tel.: +34985 18 23 69; Fax: +34985 10 43 22.

E-mail address: gutierrezantonio@uniovi.es.

## 1. Introduction

1 The sun emits energy in the form of electromagnetic radiation that travels from the sun's core to the  
2 Earth's surface. Along this pathway, solar radiation is modified mainly due to the variation in the distance  
3 between the sun and the Earth (eccentricity of the ellipse) and the attenuation processes in the  
4 atmosphere, which cause the decrease of radiation along the path [1, 2].  
5

6  
7 Accurately quantifying the incident solar radiation on a surface is a complex task that requires analyzing  
8 geometric, geographical, astronomical, physical and meteorological characteristics of the site of study.  
9 The phenomena occurring in the Earth's atmosphere are difficult to determine because the concentrations  
10 of particles and molecules present in it are highly variable. These concentrations cause the radiation  
11 attenuation processes and define the degree of cloudiness –the greater the cloudiness, the more intense the  
12 attenuation process. The parameter used to quantify the solar radiation attenuation is known as  
13 atmospheric transmittance. Transmittance of a medium is defined as the ratio between the transmitted  
14 energy and the incident one upon it. This parameter is really important in the design and implementation  
15 of large scale solar energy plants. In practice, this can be determined by using particle gauges [3] and/or  
16 mathematical models applied to meteorological measurements records.  
17

18 Du et al. reviewed scientific works on solar energy from 1992 to 2011 using bibliometric techniques  
19 based on databases of the Science Citation Index and the Social Science Citation Index [4]. Solar energy  
20 markets and policies were discussed in [5] and [6].  
21

22 As regards the quantification of solar radiation, there are three techniques to calculate its intensity: by  
23 means of instrumentation, with satellite images, and using physical and empirical irradiance models; as  
24 well as combinations of these.  
25

26 The use of instrumentation (pyranometers, pyrheliometers, heliographs, etc.) is a reliable technique;  
27 though it requires the installation of equipment for recording measurements covering large areas and long  
28 periods of time to establish a type year. It is a tedious and very expensive technique [7]. Islam et al.  
29 presented actual measurements of direct solar radiation –direct beam radiation– in Abu Dhabi with the  
30 meteorological conditions encountered during the measurement throughout the year [8, 9] Gherboudj &  
31 Ghedira assessed the solar energy potential in the United Arab Emirates using remote sensing and  
32 weather forecast data [10].  
33

34 Determining the solar radiation and the shadows effect more accurately is possible by using and  
35 processing the satellite images. However, its use is limited because of its high cost [11]. In [12], the solar  
36 energy potential of the western Himalayan Indian state of Himachal Pradesh was evaluated using an  
37 algorithm of Waikato Environment for Knowledge Analysis in Artificial Neural Network (ANN) based  
38 on a prediction model. In that paper, a correlation was developed between the NASA satellite data and the  
39 ground measured global solar radiation data to find values close to the ground measured global solar  
40 radiation for different locations. Sorapipatana [13] evaluated the solar energy potential in Thailand using  
41 a satellite technique. The results showed that the average solar radiation depends more on geographic  
42 features than on the seasonal changes.  
43

44 The utilization of physical and empirical irradiance models based on measurements and data from some  
45 regions is suitable to reliably determine solar radiation. Ertekin et al. studied solar radiation data for  
46 Antalya in Turkey. They used twenty six models to test the available data applicability for computing the  
47 monthly average daily global radiation on a horizontal surface. The models were compared on the basis of  
48 statistical error tests [14]. In [15] a review about the solar energy modeling techniques was made. They  
49 considered linear and nonlinear artificial intelligence models for solar energy prediction. El Ouderni et al.  
50 overviewed the theoretical models of solar flux estimation [16]. Copper and Sproul presented a  
51 comparative study about mathematical models in estimating solar irradiance for Australia [17].  
52

53 Sözen and Arcaklioglu investigated the effect of the relative humidity on the solar potential by using  
54 artificial neural-networks (ANN) [18]. Their results showed that the humidity has a negligible effect on  
55 the solar potential prediction. Fadare developed an ANN based on a model for the prediction of solar  
56 energy potential in Nigeria [19] and Sözen et al. used an ANN for mapping of the solar potential in  
57 Turkey [20, 21, 22]. Also, Gutierrez-Corea et al. [23] introduced a new methodology using ANN models  
58 and based on observations made in parallel by neighboring sensors and values for different variables  
59 using up to 900 inputs. The ANN models predict short-term GSI with error rates less than 20% RMSE.  
60  
61  
62  
63  
64  
65

1 The minimum difference between the average error rates obtained with these ANN models presents a  
2 1.06% RMSE improvement on average compared to previous models and studies.

3 Pan et al. [24] used the empirical Bristow–Campbell model [25] for estimating the solar radiation. In that  
4 study, the Bristow–Campbell model was validated by using daily meteorological observations over the  
5 Tibetan Plateau of China.

6  
7 Grindley et al. [26] developed a simple clear-sky irradiance model with good agreements between the  
8 predictions and measurements on a minute-by-minute basis for both the global horizontal and diffuse  
9 transmittances and those obtained under apparently clear skies. In [24], the extra-terrestrial radiation and  
10 clear sky atmospheric transmittance were calculated on a Geographic Information System (GIS) platform.

11  
12 Recently, Liu et al. [27] have studied the solar irradiance and its prediction interval are forecasted with  
13 the aid of a meteorological model for the prediction of the photovoltaic systems generation. The  
14 forecasted irradiance showed a slight positive mean bias error in the intra–day forecasting compared with  
15 the observation. Kurtz et al. [28] have measured diffuse, direct, and global irradiance using a sky imager.  
16 This technique is used for aerosol characterization, cloud detection, and solar forecasting. Global  
17 horizontal irradiance RMSE for a year-long data set is in the 9–11% range for per-image data and 6–9%  
18 for hourly-averaged data when compared against a solid-state pyranometer. A machine learning algorithm  
19 was employed by [29] to predict the horizontal sky-diffuse irradiance and conduct sensitivity analysis for  
20 the meteorological variables, but the model is based only on five years of solar irradiance measurements.  
21 A k-nearest neighbor ensemble model has been developed by [30] to generate Probability Density  
22 Function forecasts for intra-hour Direct Normal Irradiance. The proposed model is developed and  
23 validated at multiple locations with different local climates and it has high potential to benefit the  
24 integration of concentrated solar power plants.

25  
26  
27 It should be noted that there are very few models that quantify solar radiation considering the effect of the  
28 atmospheric transmittance and their use for a particular region first requires a characterization of the  
29 physical and meteorological conditions of the place under study. The treatment of all variables makes it  
30 essential to use statistical tools and mathematical methods in order to minimize calculations.

31  
32 Irradiance physical models may have limited results if the appropriate data and model are not employed.  
33 In this study, the Bird & Hulstrom model [31] is used as a base to quantify and characterize the solar  
34 resources, since it considers the elements that attenuate solar radiation passing through the atmosphere.  
35 Specifically, the non-spectral Bird & Hulstrom model, also known as model “C” of Iqbal [32, 33] has  
36 been used. This model identifies the set of coefficients responsible for the attenuation due to the presence  
37 of particles in the Earth's atmosphere.

38  
39 In this paper, a new method based on the Bird & Hulstrom model is also used to quantify solar radiation  
40 at any site according to the type of climate, altitude and state of the atmosphere. The new method  
41 significantly reduces the calculation process of the Bird & Hulstrom model and it is applied to obtain the  
42 solar energy irradiances in Mexico.

43  
44 In Mexico, the solar energy is an abundant resource [34, 35, 36, 37] although it is a country with very  
45 varying climatic conditions. There are some studies conducted by Mexican academic institutions about  
46 the solar energy potential in Mexico [38, 39, 40, 41], but the influence of physical and meteorological  
47 factors on the solar radiation is not related. Consequently, the analysis about the influence these factors is  
48 of special interest and the Bird & Hulstrom model is very suitable.

49  
50 The aim of this paper is to review the attenuation processes of the solar radiation and the analytical  
51 models for solar irradiances calculation, as well as to establish an alternative process that simplifies the  
52 Bird & Hulstrom model and computes the magnitude of overall atmospheric transmittance. This method  
53 is applied to each area of Mexico, in order to quantify and characterize the solar radiation in the whole  
54 country and it allows to identify the regions with the greatest potential for harnessing solar energy. This  
55 new methodology can be applied to any region in the world.

## 2. Attenuation processes of solar radiation

1 The energy emitted by the sun which reaches the Earth has two major features: it is scattered and  
2 intermittent. Radiation passing through the atmosphere undergoes changes which make it heterogeneous  
3 and intermittently distributed. Meteorological phenomena on Earth's atmosphere cause their variable  
4 availability [42].  
5

6 The solar radiation disposal depends on geographical, astronomical, geometrical, physical and  
7 meteorological factors. The astronomical factors are related to the solar constant, solar declination, hour  
8 angle and hours of sunshine. The geographic factors depend on the latitude, longitude and altitude of the  
9 site [43]. The geometric factors are a function of the surface height and solar azimuth angle [44]. The  
10 physical factors are related to the content of water vapor in the atmosphere, the scattering by air  
11 molecules and miscible gases, the presence of aerosols [45] and the effect of ozone [46]. Meteorological  
12 factors are related to the temperature, precipitation, humidity, etc. [47]. The latter two groups are more  
13 difficult to quantify, as they vary continuously, which make them vital factors in accurately establishing  
14 the incident energy on the Earth's surface at specific periods of time.  
15

16 The solar radiation scattering occurs when an electromagnetic wave collides with a particle and part of  
17 the incident energy is distributed in space in the form of photons which continue travelling in all  
18 directions [32]. Photons are the elements that scatter while the scattering particles are the air molecules.  
19 To determine the scattering magnitude the Rayleigh theory, which calculates the dispersion by air  
20 molecules with sizes of about 1 Å, is used [48, 33].  
21

22 The absorption of solar radiation is a process that occurs due to the presence of different components in  
23 the atmosphere and varies with the wavelength [49]. The main substances that increase absorption are the  
24 gases and particles in the air such as water vapor (H<sub>2</sub>O) and ozone (O<sub>3</sub>), as well as CO<sub>2</sub>, N<sub>2</sub>O, CO, O<sub>2</sub>,  
25 CH<sub>4</sub> and N<sub>2</sub>. Of these, only those that belong to the group known as uniformly miscible gases (CO, O<sub>2</sub>,  
26 CO<sub>2</sub>, N<sub>2</sub>O) produce significant absorption. Concentrations of CO<sub>2</sub>, CH<sub>4</sub> and N<sub>2</sub>O in the atmosphere are so  
27 low that their absorption effect is minimal and therefore can be ignored. As regards N<sub>2</sub>, despite being the  
28 most abundant gas in the atmosphere, its absorption of solar radiation is limited to a small band of the  
29 electromagnetic spectrum (X-rays and high frequencies). Therefore, its absorption is not relevant in the  
30 range of wavelengths between 0.3 and 3 µm, the range in which 96.62% of the energy of solar radiation is  
31 concentrated [50, 32].  
32

33 Other elements of significant absorption are aerosols [51, 52], either of natural origin (marine, mineral,  
34 volcanic, biogenetic and cosmic) or from human activity (dust, soot, volatile organic compounds,  
35 combustion fumes, ...) [53].  
36

37 Aerosols are heterogeneous mixtures of solid or liquid particles suspended in a gaseous medium. The size  
38 of these particles can range from 0.005 µm to 20 µm in effective radius. The influence of these substances  
39 is crucial in the attenuation process of solar radiation because:  
40

- 41 a) They give rise to the formation of clouds [54] and depending on their type and extent, they  
42 define the turbidity degree of the sky (the higher the turbidity, the higher the attenuation) [55,  
43 56].
- 44 b) They are linked to the Earth's climate, as they interact with sunlight and cause changes in the  
45 microphysical properties of clouds and their environment [57].  
46  
47

48 The presence of aerosols in the atmosphere is variable and its density defines the degree of turbidity [58].  
49 This parameter is not equal at all points of the Earth, so it must be defined for each region under study.  
50 There are several methods to do this. Some of the best known are the Angström Turbidity Coefficient and  
51 the Linke Factor [28, 59, 60].  
52

53 The magnitude of the scattering and absorption effects depends on the relative air mass, the intersection  
54 of a solar beam with the atmosphere, as well as the substances concentration in the atmosphere [34].  
55

56 To evaluate these effects it is necessary to estimate the density of each substance per unit cross section  
57 throughout the radiation path [32, 34]. Calculating these values is a complex task that requires the  
58 application of mathematical and statistical models.  
59  
60

### 3. Review of analytical models for the calculation of solar radiation

Analytical models for the solar irradiances calculation have been developed from 1940 and have been increasing in precision and complexity. This section presents a revision of the most relevant analytical models trying to gage their advantages and limitations.

#### Moon's model

In 1940 the engineer Parry Moon elaborated a pioneering model for the calculation of the direct irradiance of the whole band at sea level in which he proposed standard radiation curves [61]. He subdivided the solar spectrum into six wavelength ranges and evaluated five different solar altitude angles (90 °, 30 °, 19 °, 14 ° and 11 °). As for the characterization of the absorption and dispersion phenomena, Moon identified five different transmittances due to the dispersion of dry air, dust, ozone and dispersion and absorption by water vapor. The direct irradiation was calculated as the product of the five of them. Moon calculated the transmittance of dry air based on measurements made in 1915 by Fowle on Mount Wilson [62] with the solar spectrum wavelength ranging from 0.35 μm to 0.50 μm. The values obtained revealed that the air transmittance depends exponentially on the inverse of the wavelength fourth power. Likewise, he calculated the transmittance due to the dispersion by water vapor. To determine the transmittance due to the absorption of water vapor, Moon took the data tabulated by Fowle, obtained at an altitude of 1,730 masl [62]. As for dust transmittance, Moon formulated another exponential expression considering an average atmosphere of 800 dust particles per cm<sup>3</sup>. Finally for the transmittance due to ozone, Moon proposed an equation considering the attenuation coefficient ( $k_{o_3}$ ) previously measured by Läuchi [63].

Despite the importance of this model, as the values of dust, ozone and precipitable water level for Washington were assumed, the results obtained were only valid for this area and for the direct irradiance.

#### Reddy's model

In 1971 Reddy presented a more complex model to estimate the total daily global irradiation ( $H$ ) (Equation 1). This model introduced a notable improvement, including in its calculation the daily sun hours ( $n$ ), the average duration of the day during the month ( $N$ ), the ratio of rainy days ( $J$ ), the relative humidity ( $R$ ) and the relationship between length of day and latitude ( $K$ ) [64] [65].

$$H = K \left[ \left( 1 + 0.8 \frac{n}{N} \right) \frac{(1 - 0.2J)}{R} \right] \quad (1)$$

The model of Reddy involved a significant improvement since it introduced the climatology as a variable to estimate the global radiation of a place, but it lacked specific formulations for the calculation of direct and diffuse solar irradiation.

#### ASHRAE model

The American Society of Heating, Refrigeration and Air Conditioning Engineers (ASHRAE) published in 1972 a model to determine the solar irradiance in northern hemisphere [66]. This model is the result of the work done by Threlkeld and Jordan in 1958 [67] which is based on the technique developed by Moon for the direct radiation calculation of the entire spectral band.

To carry out the calculation of the different transmittances, they devised a basic clear atmosphere composed of 200 dust particles per cm<sup>3</sup>, an ozone concentration of 0.25 cm under normal conditions of pressure and temperature and an average monthly value of the amount of precipitable water obtained from the measurements made by Threlkeld in different parts of the United States. The values of the solar constant ( $A$ ), the optical coefficient of apparent attenuation ( $B$ ) and the relative mass of the air ( $m_r$ ) are used to estimate the direct radiation ( $G_{bn}$ ) (Equation 2).

$$G_{bn} = A e^{(-B m_r)} \quad (2)$$

The diffuse radiation ( $G_d$ ) (Equation 3) is calculated by means of a coefficient called "number of clarity" ( $C_n$ ).

$$G_d = G_{bn} C_n \quad (3)$$

The values of these parameters are tabulated for each month of a year and for a clear standard atmosphere [33]. The simplicity of this model is an advantage and it provides both direct and diffuse irradiations. However, it is only applicable to clear atmospheres.

### Lacis & Hansen model

Lacis & Hansen presented a model to estimate the global irradiance in 1973 [68]. According to Equation 4, this model determines the total irradiance as a function of the solar constant ( $G_{sc}$ ), the zenith angle ( $\theta$ ), the absorptivity of the ozone ( $a_o$ ), the absorptivity of the water vapor ( $a_w$ ), the atmospheric albedo ( $\rho'_a$ ) and the soil albedo ( $\rho_g$ ).

$$G = G_{sc}(\cos \theta) \left[ \frac{0.647 - \rho'_a - a_o}{1 - 0.0685 \rho_g} + 0.353 - a_w \right] \quad (4)$$

For the calculation of the transmittance due to the absorption of the ozone, Lacis and Hansen evaluate the absorption in two bands of the solar spectrum (the ultraviolet one and the visible one). These calculus are based on the measurements made by Manabe and Strickler [69].

This model is extremely simple and interesting because of the way in which the transmittance value due to ozone is obtained. The results indicate an overestimation of 8% in the global irradiance when the air mass is equal to 1, which is usually an acceptable value. However, it does not present a methodology for determining the direct irradiance.

### Hottel's model

In 1976 Hottel presented a new model to calculate both direct and diffuse irradiance in a "clear atmosphere" [70] [71]. The processes of absorption and dispersion that occur in the atmosphere are taken into account for the first time by means of a new coefficient named transmittance ( $\tau_b$ ). The direct radiation also depends on the solar constant ( $G_{on}$ ) and the zenith angle ( $\theta$ ) (Equation 5). This model considers four types of climates and a standard atmosphere (medium latitude and without contamination by pollution).

$$G_{cb} = G_{on} \cdot \tau_b \cdot \cos \theta \quad (5)$$

The transmittance coefficient ( $\tau_b$ ) is obtained by Equation 6:

$$\tau_b = a_0 + a_1 e^{-\left(\frac{k}{\cos \theta}\right)} \quad (6)$$

where parameters  $a_0$ ,  $a_1$  and  $k$  are defined by the climatic conditions for a standard atmosphere of 23 km of visibility (clean and clear atmosphere).

Diffuse irradiance is obtained by Equation 7:

$$G_{cd} = G_{on} \cdot \tau_d \cdot \cos \theta \quad (7)$$

where  $\tau_d$  is the transmittance coefficient for the diffuse component and is given by Equation 8:

$$\tau_d = 0.2710 - 0.2939 \cdot \tau_b \quad (8)$$

This model is interesting for its simplicity, but it only applies to clear atmospheres.

### Davies & Hay model

In 1978 Davies and Hay presented in the First Canadian Solar Radiation Data Workshop a model for the calculation of both direct ( $G_b$ ) and diffuse irradiance ( $G_{as}$ ) [72]. The model also considers the fraction of irradiance due to the multiple reflections between the soil and the atmosphere ( $G_{dm}$ ). The global irradiance ( $G_{mdh}$ ) is given by the sum of these three solar components (Equation 9).

$$G(MDH) = G_b(MDH) + G_{as}(MDH) + G_{dm}(MDH) \quad (9)$$

The direct irradiance ( $G_b$ ) is calculated as a function of the solar constant, the zenith angle, the transmittance due to the presence of precipitable water vapor, and the transmittances due to the absorption of ozone, the aerosol dispersion and the air molecules.

The transmittance due to the absorption of the ozone depends on the optical depth of the ozone.

For the transmittance due to the presence of aerosols, Davies and Hay introduce a new factor ( $k_{MDH}$ ) representing the characteristics of an aerosol. The transmittance due to the absorption of water vapor depends on the optical depth of the precipitable water.

The diffuse irradiance ( $G_{as}$ ) contemplates the analysis of the dispersion of the aerosols by albedo ( $\omega_o = 0.98$ ), as well as the aerosol forward scattering ratio ( $F_c$ ), which is the percentage of energy due to the dispersion by aerosols that is directed towards the Earth's surface ( $F_c = 0.85$ ). Finally, the fraction of the diffuse irradiance due to the multiple reflections between the sky and the atmosphere is considered ( $G_{dm}$ ). This irradiance is calculated from the albedos of the soil and the atmosphere.

This model significantly improves the previous ones and was the first one to treat the direct and diffuse irradiance separately. Its limitations were that it does not present a method for the treatment of the transmittance of aerosols and that it requires tabulated values for the effects produced by air molecules.

### Hoyt's model

Also in 1978, Hoyt published a model for the calculation of the global irradiance ( $G_{global}$ ) from the sum of direct irradiance ( $G_b$ ) and diffuse irradiance. The latter is determined by two effects: the aerosol dispersion ( $G_{dra}$ ) and multiple reflections between soil and atmosphere ( $G_{dm}$ ) [73] (Equation 10).

$$G_{global} = G_b + G_{dra} + G_{dm} \quad (10)$$

Hoyt proposed different expressions to determine each component from the analysis of different radiation sources, such as water vapor, carbon dioxide, ozone, oxygen and aerosols. For the calculation of direct irradiance ( $G_b$ ), Hoyt proposed an equation including the solar constant ( $G_{sc}$ ), zenith angle ( $\theta$ ), and dispersion by aerosols ( $\tau_{as}$ ) and by pure air ( $\tau_r$ ) (Equation 11).

$$G_b = G_{sc} \cos \theta \left( 1 - \sum_{i=1}^5 a_i \right) \tau_{as} \tau_r \quad (11)$$

where ( $a_i$ ) is a one-factor term for each of the above mentioned attenuation sources.

The evaluation of the transmittance due to the presence of water vapor ( $a_1$ ) is based on values obtained by Yamamoto [74]. The transmittance due to the presence of carbon dioxide ( $a_2$ ) is calculated from the values obtained by Burch [75]. For the transmittance due to the absorption of ozone ( $a_3$ ), Hoyt establishes an equation based on the works of Manabe and Strickler [69]. The calculation of the transmittance due to the presence of molecules such as oxygen ( $a_4$ ) is referred to the mass of air corrected by pressure ( $m_a$ ). Finally, to evaluate the transmittance due to aerosol absorption ( $a_5$ ), tabulated values of the turbidity coefficient of Angstrom [76] [77] are used. To do that, Hoyt introduces a novel analysis which considers the aerosol dispersion behavior depending on the turbidity coefficient of Angstrom. Hoyt proposes Equation 12 for the transmittance due to the dispersion by air molecules.

$$\tau_r = \left[ f(m_a) \right]^{m_a} \quad (12)$$

where parameter  $f(m_a)$  is tabulated as a function of the mass of air corrected by pressure ( $m_a$ ) [73].

The diffuse irradiance is calculated by adding two mentioned terms ( $G_{dra} + G_{dm}$ ), aerosol dispersion ( $G_{dra}$ ) (Equation 13) and multiple reflections between soil and atmosphere ( $G_{dm}$ ) (Equation 14). For the latter, the value of the atmospheric albedo ( $\rho_g$ ) is used.

$$G_{dra} (Hoyt) = G_{sc} \cos \theta \left( 1 - \sum_{i=1}^5 a_i \right) \left[ (1 - \tau_r) 0.5 + (1 - \tau_{as}) 0.75 \right] \quad (13)$$

$$G_{dm} (Hoyt) = (G_b + G_{dra}) \rho_g \left[ 1 - \sum_{i=1}^5 a'_i \right] \left[ (1 - \tau'_r) 0.5 + (1 - \tau'_{as}) 0.25 \right] \quad (14)$$

This model is one of the most complete, however it has the disadvantage that its application is tedious and some of the values are calculated from tabulated data of reference regions. That is the reason why the application of Hoyt's model has been restricted to places where no information on atmospheric components is available.

### Atwater & Ball model

In 1978 M.A. Atwater & J.T. Ball presented a rigorous model for the direct irradiance ( $G_b$ ) and also evaluated the diffuse irradiance [78]. A clear sky equivalent to a visibility of 23 km (extreme clarity) was

considered to calculate the direct irradiance (Equation 15) which depends on the solar constant ( $G_{sc}$ ), the zenith angle ( $\theta$ ) and the transmittances due to the molecular effects ( $\tau_b$ ), water vapor ( $a_w$ ) absorption and aerosols ( $\tau_a$ ).

$$G_b = G_{sc} (\cos \theta) (\tau_b - a_w) \tau_a \quad (15)$$

In order to determine the transmittance of all molecular effects ( $\tau_b$ ), the model is based on the analysis made by McDonald [79] which does not include the transmittance due to the absorption of water vapor. The presence of ozone is not evaluated individually. It is included into the general molecular effects.

The global irradiance is obtained taking into account the soil and atmospheric albedos. The latter is considered equal to 0.0685, which is the value obtained by Lacis and Hansen for a clear atmosphere.

In spite of its rigor and simplicity, this model is limited to atmospheric conditions of extreme clarity, since it does not consider the transmittance due to the presence of aerosols. It is not applicable for skies with turbidity.

### Watt's model

Another of the solar models published in 1978 was Watt's model [80]. This author developed a methodology for the calculation of direct and diffuse irradiance based on Moon's studies.

The direct irradiance ( $G_b$ ) depends on the solar constant ( $G_{sc}$ ) and the zenith angle ( $\theta$ ). Watt considered the attenuating effects of the different transmittances: absorption of water vapor ( $\tau_{wa}$ ), absorption and dispersion of dry air ( $\tau_{AS}$ ), absorption of ozone ( $\tau_o$ ), absorption and dispersion of aerosols in the entire radiation spectrum for both low ( $\tau_{aL}$ ) and high layers ( $\tau_{aU}$ ) of the earth's atmosphere. He also considered the dispersion by water vapor ( $\tau_{ws}$ ) (Equation 16).

$$G_b = G_{sc} \cos \theta \tau_{wa} \tau_{AS} \tau_o \tau_{ws} \tau_{aL} \tau_{aU} \quad (16)$$

An empirical expression to calculate the transmittance due to water absorption was obtained using the data recorded in the Handbook of Geophysics and Space Enviroments [81] with good results. In this model, Watt included the analysis of the optical depth which he called "path length modifiers", a similar concept to the mass of air, depending on the components (dry air, water vapor, aerosols and ozone) and the altitude.

Finally, for the calculation of the diffuse irradiance, Watt considered all the scattering effects occurring in the atmosphere, the atmospheric and the soil albedos.

This is a rigorous complete model based on meteorological parameters, allowing reliable results. The values of global radiation obtained are overestimated by 7% for air masses equal to 1. The application is complex because it requires data like the turbidity of aerosols in the upper layers of the atmosphere, which are difficult to obtain. However, it represents an important advance in the analysis of radiation.

### Bird & Hulstrom model and improvements

The non-spectral Bird & Hulstrom model (1981) or model "C" of Iqbal [34] is more complete and accurate than the models previously presented and it is explained in more detail. This model determines the total irradiance ( $I_{TH}$ ), from the amount of direct irradiance ( $I_{DH}$ ) and diffuse irradiance ( $I_{dH}$ ) on a horizontal surface for the entire frequency band [82] (Equation 17).

$$I_{TH} = I_{DH} + I_{dH} \quad (17)$$

The direct irradiance ( $I_{DH}$ ) on a horizontal surface is determined from Equation 18.

$$I_{DH} = 0.9662 \cdot C_r \cdot \tau_r \cdot \tau_o \cdot \tau_g \cdot \tau_w \cdot \tau_a \cdot \text{sen}A \quad (18)$$

being:

$C_r$ : Value of daily solar constant ( $\text{W/m}^2$ ).

$\tau_r$ : Transmittance by scattering due to air molecules.

$\tau_o$ : Transmittance due to absorption of ozone ( $\text{O}_3$ ).



1  $\tau_g$ : Transmittance due to absorption by the uniform gases mixture (CO<sub>2</sub> and O<sub>2</sub>).

2  $\tau_w$ : Transmittance due to absorption of water vapor.

3  $\tau_a$ : Transmittance due to absorption and scattering by the presence of aerosols.

4 0.9662: Correction factor which adjusts the wavelength range of the solar spectrum (0.3 to 3  $\mu\text{m}$ ).

5 A: solar altitude angle in degrees.

6 The position of the sun relative to a point on the Earth's surface has an angle of incidence with reference  
7 to the horizontal plane at the same point which is called the solar altitude angle (A).

8  
9 The value of the daily solar constant varies according to Equation 19[34].

$$11 \quad C_r = C \cdot \left( 1 + 0.033 \cdot \cos \frac{360 \cdot n}{365} \right) \quad (19)$$

12 where  $n$  is the Julian day and  $C$  is the normalized solar constant,  $C = 1367 \text{ W/m}^2$  (average annual solar  
13 radiation arriving at the outer limits of the Earth's atmosphere).

14  
15 The transmittance by scattering ( $\tau_r$ ) evaluates the change of direction experienced by solar radiation due  
16 to the presence of air molecules (Equation 20).

$$17 \quad \tau_r = e^{-0.0903 m_a^{0.84} (1 + m_a - m_a^{1.01})} \quad (20)$$

18 where  $m_a$  is the optical air mass [34], which depends on the total air pressure ( $P_T$ ), the relative air mass  
19 ( $m_{rel}$ ), the solar altitude angle (A) and the altitude (z).

20 The transmittance due to the absorption of ozone ( $\tau_o$ ) depends on the relative air mass and the thickness  
21 of the ozone layer ( $Lo$ ) of the atmosphere [34] (Equation 21).

$$22 \quad \tau_o = 1 - \left[ 0.1611 \cdot \left[ (Lo \cdot m_{rel}) (1 + 139.48 \cdot Lo \cdot m_{rel})^{-0.3035} \right] + \frac{0.002715 \cdot Lo \cdot m_{rel}}{1 + 0.044 \cdot Lo \cdot m_{rel} + 0.003 \cdot (Lo \cdot m_{rel})^2} \right] \quad (21)$$

23  
24 The transmittance due to absorption by the uniform gases mixture ( $\tau_g$ ) is determined by Equation 22  
25 [34].

$$26 \quad \tau_g = e^{-0.0127 m_a^{0.26}} \quad (22)$$

27 The transmittance due to absorption of water vapor ( $\tau_w$ ) is obtained from Equation 23 [34].

$$28 \quad \tau_w = 1 - \frac{2.4959 \cdot (WW \cdot m_{rel})}{(1 + 79.034 \cdot WW \cdot m_{rel})^{0.6828} + 6.385 \cdot WW \cdot m_{rel}} \quad (23)$$

29  $WW$  being the amount of water capable of precipitating vertically [34].

30 Finally, it was found that aerosols have a strong impact on the atmospheric turbidity [83]. The influence  
31 of radiation is important because it can absorb or scatter the incident photons depending on the size of the  
32 aerosol.

33 Mächler parameterization [84] is used to obtain the transmittance due to the presence of aerosols ( $\tau_a$ ),  
34 according to the Iqbal model (Equation 24). This parameterization depends on the average particle size  
35 ( $\alpha$ ) and the amount of aerosols. The average particle size is  $1.3 \mu\text{m} \pm 0.2$  [85]. The amount of aerosols is  
36 measured by the degree of turbidity of the atmosphere ( $\beta$ ). This parameter is also called the Angstrom  
37 turbidity coefficient and can vary from 0 (extremely clean atmospheres) to 0.5 (extremely turbid  
38 atmospheres).

$$\tau_a = 0.12445 \cdot \alpha - 0.0162 + (1.003 - 0.125 \cdot \alpha) \cdot e^{-\beta \cdot m_a (1.089 \alpha + 0.5123)} \quad (24)$$

The product of all attenuation coefficients responsible for direct radiation ( $\tau_r$ ,  $\tau_o$ ,  $\tau_g$ ,  $\tau_w$  and  $\tau_a$ ) is called atmospheric overall transmittance of direct radiation ( $\tau_{total}$ ).

The total diffuse irradiance on a horizontal surface is made up of to three solar components [34] (Equation 25):

- Due to scattering by air molecules (Rayleigh diffusion) ( $I_{dr}$ ).
- Due to the existence of dust particles (aerosols) ( $I_{da}$ ).
- Caused by multiple reflections between the ground and the atmosphere ( $I_{dm}$ ).

$$I_{dH} = I_{dr} + I_{da} + I_{dm} \quad (25)$$

Diffuse irradiance due to the existence of air molecules is obtained from Equation 26.

$$I_{dr} = 0.79 \cdot C_r \cdot \tau_o \cdot \tau_g \cdot \tau_w \cdot \tau_{aa} \cdot 0.5 \cdot \frac{1 - \tau_r}{1 - m_a + m_a^{1.02}} \cdot senA \quad (26)$$

This model assumes that 50% of solar energy is directed toward the Earth's surface due to scattering by air molecules. The transmittance due to absorption by aerosols ( $\tau_{aa}$ ) (Equation 27) requires the scattering albedo ( $\omega_o$ ) whose value is 0.9 [31].

$$\tau_{aa} = 1 - (1 - \omega_o)(1 - m_a + m_a^{1.06})(1 - \tau_a) \quad (27)$$

The diffuse radiation due to the presence of aerosols is obtained from Equation 28.

$$I_{da} = 0.79 \cdot C_r \cdot \tau_o \cdot \tau_g \cdot \tau_w \cdot \tau_{aa} \cdot F_c \cdot \frac{1 - \tau_{as}}{1 - m_a + m_a^{1.02}} \cdot senA \quad (28)$$

being:

$F_c$ : percentage of the energy on the Earth's surface due to scattering by aerosols, estimated from Mac's parametrization (Equation 29).

$$F_c = 0.93 - 0.21 \ln m_a \quad (29)$$

$\tau_{as}$ : transmission coefficient due solely to diffusion by aerosols, obtained from Equation 30.

$$\tau_{as} = \frac{\tau_a}{\tau_{aa}} \quad (30)$$

The calculation of diffuse irradiance by multiple reflections ( $I_{dm}$ ) requires the reflection coefficients of each different surface ( $\rho_g$ ). It also requires an evaluation of the atmospheric albedo, ie, multiple reflections between the ground and the sky ( $\rho'_a$ ) [29] (Equations 31 and 32).

$$I_{dm} = (I_{dH} \cdot senA + I_{dr} + I_{da}) \cdot \frac{\rho_g \cdot \rho'_a}{1 - \rho_g \cdot \rho'_a} \quad (31)$$

$$\rho'_a = 0.0685 + (1 - F_c)(1 - \tau_{as}) \quad (32)$$

As it can be seen, the application of the Bird & Hulstrom model assesses the influence of climatic and meteorological variables, which are responsible for the attenuation of solar radiation, giving very reliable results.

#### 4. Methodology

In this study, a new method is developed based on the non-spectral Bird & Hulstrom model, which is the most complete and accurate of the analytical models presented in the previous section. The new method interpolates the values obtained by Bird & Hulstrom model by means of very simple equations which allow to quantify the solar irradiances at any site according to the type of climate, altitude and state of the atmosphere. This method significantly reduces the calculation process.

As a study case it is applied to Mexico where, to obtain the specific parameters, data from several weather stations along the country were used.

##### 4.1 Data acquisition and processing: Weather stations

74 weather stations located in different parts of the country [86] were used to acquire the meteorological information of the different climates of Mexico.

The daily average records of variables such as temperature, sunshine hours, humidity, evaporation, altitude, barometric pressure and rainfall within a period of 20 years were obtained for each weather station. These data are enough to develop the model proposed. Table 1 shows the mean characteristics of the weather stations [86]. Altitude is expressed in meters above sea level (masl).

Table 1. Weather stations in Mexico

No.	Station	State	Latitude	Longitude	Altitude (masl)	Temperature (°C)	Relative Humidity (%)
1	Acapulco	Guerrero	16°45'47"	99°44'56"	3	28	0.75
2	Aguascalientes	Aguascalientes	21°51'12"	102°17'29"	1877	19	0.52
3	Altar	Sonora	30°42'52"	111°50'05"	397	22	0.56
4	Arriaga	Chiapas	16°14'28"	93°53'51"	49	28	0.72
5	Campeche	Campeche	19°50'	90°30'	5	27	0.72
6	Chetumal	Quintana Roo	18°29'	88°18'	9	27	0.77
7	Chihuahua	Chihuahua	28°42'	106°07'	1482	19	0.5
8	Chilpancingo	Guerrero	17°33'	99°30'	1265	23	0.67
9	Ciudad Guzmán	Jalisco	19°43'50"	103°27'53"	1515	20	0.66
10	Ciudad Victoria	Tamaulipas	23°44'52"	99°10'18"	336	25	0.71
11	Coatzacoalcos	Veracruz	18°11'22"	94°30'39"	16	26	0.78
12	Colima	Colima	19°14'32"	103°43'13"	444	26	0.58
13	Colotlán	Jalisco	22°06'26"	103°16'04"	1736	19	0.55
14	Comitán	Chiapas	16°14'	92°08'	1607	19	0.71
15	Cozumel	Quintana Roo	20°31'	86°56'	4	26	0.8
16	Cuernavaca	Morelos	18°53'32"	99°14'	1618	21	0.57
17	Culiacán	Sinaloa	24°38'05"	107°26'26"	39	25	0.49
18	Durango	Durango	24°05'41"	104°35'59"	1872	18	0.64
19	Empalme	Sonora	27°57°	110°48'	12	25	0.59
20	Felipe Carrillo	Quintana Roo	19°34'	88°03'	10	26	0.76
21	Guadalajara	Jalisco	20°42'36"	103°23'24"	1551	20	0.61
22	Guanajuato	Guanajuato	21°00'20"	101°17'08"	1999	19	0.63
23	Hermosillo	Sonora	29°04'42"	110°55'48"	211	22	0.66
24	Hidalgo	Chihuahua	26°55'	105°40'	1785	18	0.57
25	Huajuapán	Oaxaca	17°48'	97°46'	1680	19	0.62
26	Isla	Colima	18°43'	110°57'	34	25	0.71
27	Jalapa	Veracruz	19°30'43"	96°54'14"	1360	19	0.46
28	La Paz	BCS	24°07'	110°9'	19	25	0.6
29	Lagos Moreno	Jalisco	21°20'44"	101°56'40'	1920	19	0.59
30	Loreto	BCS	26°01'	111°20'	7	24	0.66

31	Manzanillo	Colima	19°04'	104°20'	3	27	0.75
32	Matlapa	San Luís Potosí	21°20'	98°50'	133	24	0.79
33	Mazatlán	Sinaloa	23°14'	106°24'	3	25	0.74
34	Mérida	Yucatán	20°57'	89°39'	11	25	0.7
35	Monclova	Coahuila	26°54'30"	101°25'	615	20	0.48
36	Monterrey	Nuevo León	25°44'11"	100°18'17"	515	23	0.65
37	Morelia	Michoacán	19°42'	101°11'	1913	19	0.58
38	Nacozari	Sonora	30°22'	109°41'	1040	13	0.48
39	Nuevo casas	Chihuahua	30°22'	107°57'	1468	17	0.49
40	Oaxaca	Oaxaca	17°04'	96°42'	1519	21	0.64
41	Obregón	Sonora	27°29'	109°55'	38	25	0.69
42	Orizaba	Veracruz	18°51'	97°06'	1259	18	0.78
43	Pachuca	Hidalgo	20°07'42"	98°44'51"	2425	15	0.61
44	Piedras Negras	Coahuila	28°42'	100°31'	250	23	0.52
45	Progreso	Yucatán	21°16'33"	89°39'14"	2	26	0.7
46	Puebla	Puebla	19°03'	98°10'	2179	16	0.58
47	Puerto Ángel	Oaxaca	15°39'	96°29'	43	27	0.74
48	Puerto Peñasco	Sonora	31°18'03"	113°32'55"	61	22	0.63
49	Querétaro	Querétaro	20°35'	100°24'	1881	19	0.56
50	Río Verde	San Luís Potosí	21°55'17"	99°59'47"	984	22	0.65
51	Salina Cruz	Oaxaca	16°10'15"	95°10'45"	2	28	0.62
52	Saltillo	Coahuila	25°22'35"	101°10'	1790	18	0.6
53	San Cristóbal	Chiapas	16°44'	92°38'	2115	15	0.82
54	San Luís	San Luís Potosí	22°12'27"	101°01'20"	1883	18	0.59
55	Santa Rosalía	BCS	27°17'	112°15'	82	24	0.57
56	Sombrerete	Zacatecas	23°28'	103°39'	2351	16	0.54
57	Soto la Marina	Tamaulipas	23°46'	98°12'	21	26	0.65
58	Tacubaya	México DF	19°24'13"	99°11'46"	2309	18	0.57
59	Tampico	Tamaulipas	22°12'	97°51'22"	25	25	0.78
60	Tamuín	San Luís Potosí	22°01'	98°47'01"	23	26	0.69
61	Tapachula	Chiapas	14°55'15'	92°15'	118	27	0.74
62	Temosachic	Chihuahua	28°57'	107°49'	1932	12	0.65
63	Tepehuanes	Durango	25°20'16"	105°43'23"	1810	16	0.56
64	Tepic	Nayarit	21°29'21"	104°53'35"	915	22	0.71
65	Tlaxcala	Tlaxcala	19°18'43"	98°14'39"	2248	16	0.72
66	Toluca	México DF	19°17'	99°39'	2663	12	0.65
67	Torreón	Coahuila	25°31'11"	103°25'52"	1123	22	0.5
68	Tuxpan	Veracruz	20°57'35"	97°25'08"	10	25	0.82
69	Tuxtla	Chiapas	16°45'	93°08'	570	26	0.64
70	Valladolid	Yucatán	20°41'24"	88°12'15"	27	27	0.74
71	Veracruz	Veracruz	19°09'40"	96°08'13"	20	25	0.78
72	Villahermosa	Tabasco	17°59'	92°56'	7	25	0.75
73	Zacatecas	Zacatecas	22°46'42"	102°33'59"	2612	16	0.54
74	Zamora	Michoacán	19°59'	102°19'	1562	16	0.59

These stations provide information about the five types of climates predominant in Mexico (warm-humid, sub-humid warm, dry, very dry and sub-humid mild). Weather stations have been classified and located on the digital map of the National Institute of Statistics and Geography [87] (Figure 1).

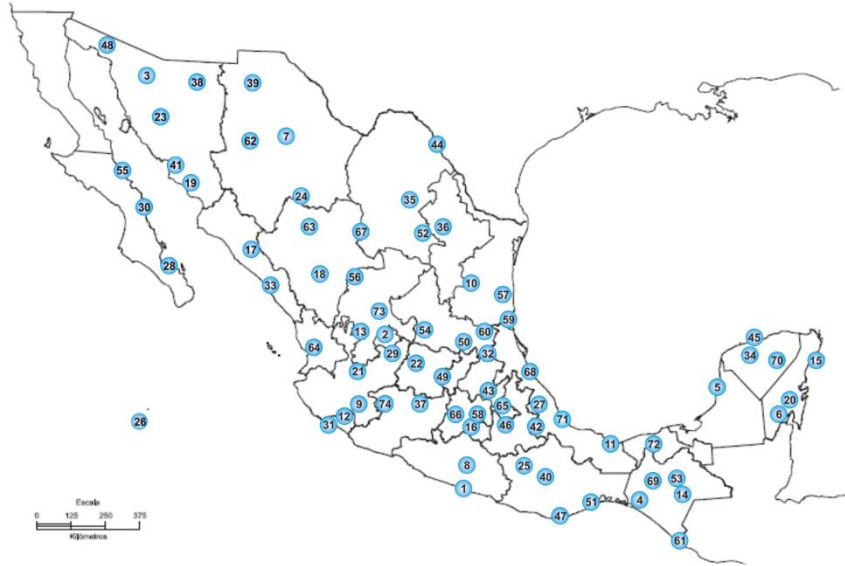


Figure 1. Location of weather stations

#### 4.2 New Proposed Method: Simplification of the Bird & Hulstrom Model

Obtaining solar data using the Bird & Hulstrom model is a complex process requiring information about the hypsography, climate and meteorology which is often unavailable. In this paper, a user-friendly method with high accuracy is developed. The Bird & Hulstrom model is used as a base, incorporating the adjustments made by Mächler, Leckner, Mac and Iqbal explained in the previous section. Thus, the total solar irradiance ( $I_{TH}$ ) is the sum of direct ( $I_{DH}$ ) and diffuse irradiance ( $I_{dH}$ ) on a horizontal surface (Equation 17).

##### 4.2.1 Direct solar irradiance on a horizontal surface ( $I_{DH}$ )

The direct irradiance ( $I_{DH}$ ) is obtained by multiplying the amount of energy from the sun by its position relative to a point on the Earth's surface. Equation 33 is obtained considering that the incident solar energy on the upper layers of the atmosphere is  $C = 1367 \text{ W/m}^2$  (solar constant) and the sun's position is determined by means of the solar altitude angle ( $A$ ).

$$I_{DH} = C \cdot \text{sen}A \quad (33)$$

$I_{DH}$  obtained from the above equation is imprecise, since it does not take into account that wavelength ranges from  $0.3$  to  $3 \mu\text{m}$  nor the mitigating effect of radiation passing through a medium. This effect depends on the optical air mass and the processes of absorption and scattering.

The optical air mass is determined from the relative air mass ( $m_{rel}$ ), while absorption and scattering processes are quantified from the calculation of the different transmittances. For this reason, it is necessary to define a new coefficient of atmospheric transmittance ( $\tau_{OAT}$ ) so that all of these variables can be used establish a global attenuation coefficient, as stated by Moon [61]. Taking into account those considerations, Equation 33 can be rewritten as Equation 34, which gives much more accurate values for  $I_{DH}$ .

$$I_{DH} = 0.9662 \cdot C \cdot \tau_{OAT} \cdot \text{sen}A \quad (34)$$

being:

$C$ : The solar constant.

- A: Solar altitude angle in degrees.  
 0.9662: Correction factor which adjusts the wavelength range of the solar spectrum (0.3 to 3  $\mu\text{m}$ ).  
 $\tau_{OAT}$ : Overall atmospheric transmittance.

Equation 34 significantly reduces the calculation process of the Bird & Hulstrom model, however, it requires the overall atmospheric transmittance for Mexico. To do so, it is necessary to know the turbidity degree of the atmosphere ( $\beta$ ) observed in recent years for the city of Mexico. According to Jáuregui [88], it ranges between 0.2 and 0.4, but when the polar air mass crosses it in dry seasons, the winds associated wash away some of the pollutants and solar radiation reaches the Earth's surface without suffering significant attenuation. For this reason, values of  $\beta$  between 0.0 and 0.4 have been taken [89]. Table 2 shows the relationship between the type of atmosphere and the turbidity degree.

Table 2. Relationship between type of atmosphere and the turbidity degree

$\beta$	Type of atmosphere
0.0	Extremely clean
0.1	Clear
0.2	Slightly turbid
0.3	Turbid
0.4	Very turbid

#### 4.2.2 Diffuse solar irradiance on a horizontal surface ( $I_{dH}$ )

The diffuse solar irradiance ( $I_{dH}$ ) calculation is more complex than direct solar irradiance, since it requires knowledge of the multiple reflections between the Earth and the atmosphere. This calculation needs to resort to the meteorological observations. In this model, the diffuse irradiance on a horizontal surface depends on the clear sky index ( $k_d$ ) as this has been proved to give satisfactory results [90]. Therefore, this irradiance is given by Equation 35.

$$I_{dH} = C \cdot k_d \cdot \text{sen}A \quad (35)$$

The clear sky index is defined by a diffuse atmospheric coefficient, which is given by the transmittances that affect only diffuse radiation. In these terms, there are several studies which define clarity of the sky corresponding to the diffuse sky fraction as a linear function of an overall atmospheric transmittance [91, 92, 93, 94]. The correlations made by these authors and their results provide evidence that this methodology is perfectly acceptable. Consequently, the clear sky index ( $k_d$ ) can be expressed by Equation 36, where  $B$  and  $B'$  are parameters that must be determined by a statistical analysis of a place weather conditions [95].

$$k_d = B - B' \cdot \tau_{OAT} \quad (36)$$

Parameter  $B$  is the maximum value of the clear sky index (minimum reflections between the soil and the atmosphere) and  $B'$  quantifies how this index varies due to attenuation processes of solar radiation in the atmosphere. In order to obtain the clear sky index, it is necessary to determine the overall atmospheric transmittance.

#### 4.2.3 Overall atmospheric transmittance ( $\tau_{OAT}$ )

To determine the overall attenuation coefficient, Beer's Law is taken into account [96]. This law, applied to solar radiation, establishes that the coefficient of atmospheric transmissibility for direct radiation decreases with the content of particles contained in the atmosphere and the path length of solar radiation [97]. Therefore this coefficient can be expressed by Equation 37.

$$\tau_{OAT} = a \cdot e^{-(b \cdot m_{rel})} \quad (37)$$

where  $a$  and  $b$  are parameters for the place of study which define the degree of attenuation experienced by solar radiation in that place and  $m_{rel}$  is the relative air mass.

Parameter  $a$  represents the flux density of solar radiation ( $W/m^2$ ) when solar beams enter the atmosphere (maximum value).

Parameter  $b$  also called the “attenuation coefficient”, is the probability of a solar ray being intercepted at a point within the atmosphere [96].

The relative air mass ( $m_{rel}$ ) is a purely geometrical relation that evaluates the intersection of a solar beam with the atmosphere, considering the curvature of the Earth.

For solar altitude angles ranging between  $30^\circ$  and  $90^\circ$  the equation to obtain  $m_{rel}$  [34] can be simplified as shown in Equation 38.

$$m_{rel} = \frac{1}{\sin A + 0.15[93.885 - (90 - A)]^{-1.253}} \approx \frac{1}{\sin A} \quad (38)$$

Consequently, Equation 39 is obtained.

$$\tau_{OAT} = a \cdot e^{-\left(\frac{b}{\sin A}\right)} \quad (39)$$

#### 4.2.4 Obtaining the new model parameters.

Obtaining  $\tau_{OAT}$  from Equation 39 requires the calculation of parameters  $a$  and  $b$ . To do so, a correlation analysis by the least squares method between the product of the atmospheric transmittances

( $\tau_r \cdot \tau_o \cdot \tau_g \cdot \tau_w \cdot \tau_a$ ) and the position of the sun (solar altitude angle) at each weather station is done.

This involves the calculation of the relative air mass ( $m_{rel}$ ). The product of those transmittances obtained by the Bird & Hulstrom method is denoted  $\tau_{total}$ .

In making this correlation, exponential curves confirming Beer's Law are obtained for each weather station and type of atmosphere.  $\tau_{total}$  decreases exponentially with the length traveled by the solar beams, that is, the lower the solar altitude angle, the greater the solar attenuation (Figure 2).

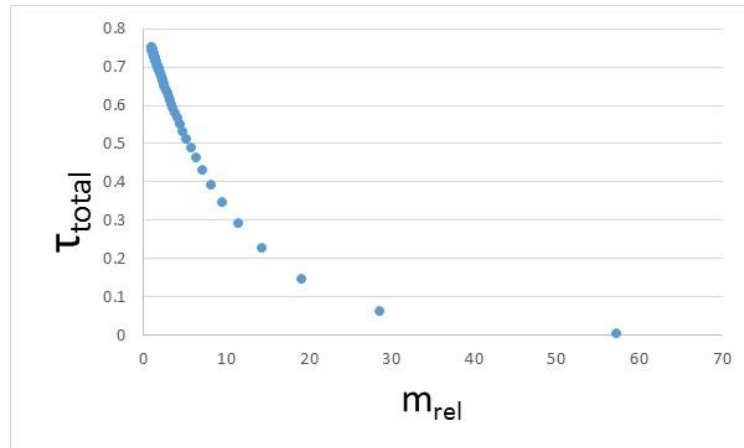


Figure 2. Correlation curve between the total transmittance and the relative air mass

By means of these correlations and considering  $\tau_{total} = \tau_{OAT}$ , parameters  $a$  and  $b$  can be obtained by least square fitting.

According to the Bird & Hulstrom method and rearranged the Equations from 9 to 16, a new transmittance can be defined (diffuse global transmittance:  $\tau_{diff}$ ), obtaining Equation 40, equivalent to Equation 35.

$$I_{dH} = C \cdot \tau_{diff} \cdot senA \quad (40)$$

To calculate the values of parameters  $B$  and  $B'$  it is necessary to determine the diffuse global transmittance, which is given by the transmittances that affect only the diffuse radiation.

Correlation analyses between the diffuse global transmittance ( $\tau_{diff}$ ) and the overall atmospheric transmittance ( $\tau_{OAT}$ ) for each weather station and type of atmosphere result in a set of straight lines with negative slope. The correlation obtained between the two parameters is linear and very similar to the correlations proposed by Spencer [94].

Considering that the clear sky index ( $k_d$ ) equals diffuse global transmittance ( $\tau_{diff}$ ), parameters  $B$  and  $B'$  can be obtained by least square fitting (Equation 41).

$$\tau_{diff} = B - B' \cdot \tau_{OAT} \quad (41)$$

## 5. Results and analysis

Monthly average data from the Mexican weather stations were used to obtain atmospheric transmittances ( $\tau_r$ ,  $\tau_o$ ,  $\tau_g$  and  $\tau_w$ ) using the Bird & Hulstrom model. Transmittance due to aerosols ( $\tau_a$ ) depends on the different types of atmospheric turbidity quantified by the turbidity degree ( $\beta$ ). This procedure was performed for all the weather stations and types of atmosphere to obtain a monthly average of  $\tau_{total}$ . Similarly, the values relative to astronomical, geometrical and geographical factors, including the corresponding solar altitude and the relative air mass, were taken into account for each weather station and type of atmosphere, as they are necessary for the development of the proposed correlation system.

### 5.1 Direct Solar Irradiance Parameters

Mean Solar altitud angles in Mexico are greater than  $35.6^\circ$ , therefore the data meet the restriction set for equation 38. The different exponential correlations  $\tau_{OAT}$  versus  $m_{rel}$  were obtained for each weather station and type of atmosphere, as well as the respective values of both parameters  $a$  and  $b$ . The coefficients of determination ( $R^2$ ) obtained to evaluate the goodness-of-fit were greater than 0.99, indicating that the results are fully satisfactory.

Grouping the weather stations according to the type of climate in Mexico (warm-humid, sub-humid warm, dry, very dry and sub-humid mild), the average values of parameters  $a$  and  $b$  for each climate and the type of atmosphere were obtained, as well as the overall atmospheric transmittances ( $\tau_{OAT}$ ). The coefficients of determination ( $R^2$ ) obtained for some climates were less than 0.85, indicating that the results are not very good. Using those values, direct solar irradiances ( $I_{DH}$ ) were obtained and compared to the values obtained by the Bird & Hulstrom model. Discrepancies were up to 12%, therefore it can be concluded that climate factor alone is not determinant.

As the weather stations are located in different areas of Mexico, some at the sea level and others in high mountain areas, it was concluded that altitudes might be also influence the computation. The path gone through more air mass (atmosphere) is lower than in those stations located in higher altitudes, so that solar radiation is attenuated to a lesser extent than in stations located at sea level. Thus, the country hypsography from the information displayed by the Institute of Geography of the UNAM [98] was assessed. Weather stations were re-classified by climate and altitude intervals (0-1000 masl, 1000-2000 masl and greater than 2000 masl) and new values of the parameters  $a$  and  $b$  were obtained. The values of these parameters, their dispersion in the territory and their relationship to the climate are described below.

Figures 3 and 4 show the values of the overall atmospheric transmittance ( $\tau_{OAT}$ ) and diffuse global transmittance ( $\tau_{diff}$ ) versus solar altitude ( $A$ ) for the group of stations corresponding to the sub-humid warm climate, altitude interval 1000-2000 masl and very turbid atmosphere ( $\beta=0.4$ ), as an example. In those figures is also represented the curve obtained by least square fitting (New method).



Similar results were obtained for the other groups of stations. The statistical values obtained indicate that this new classification is correct. In all cases the coefficients of determination ( $R^2$ ) obtained for each climate, altitude interval and turbidity degree were greater than 0.99.

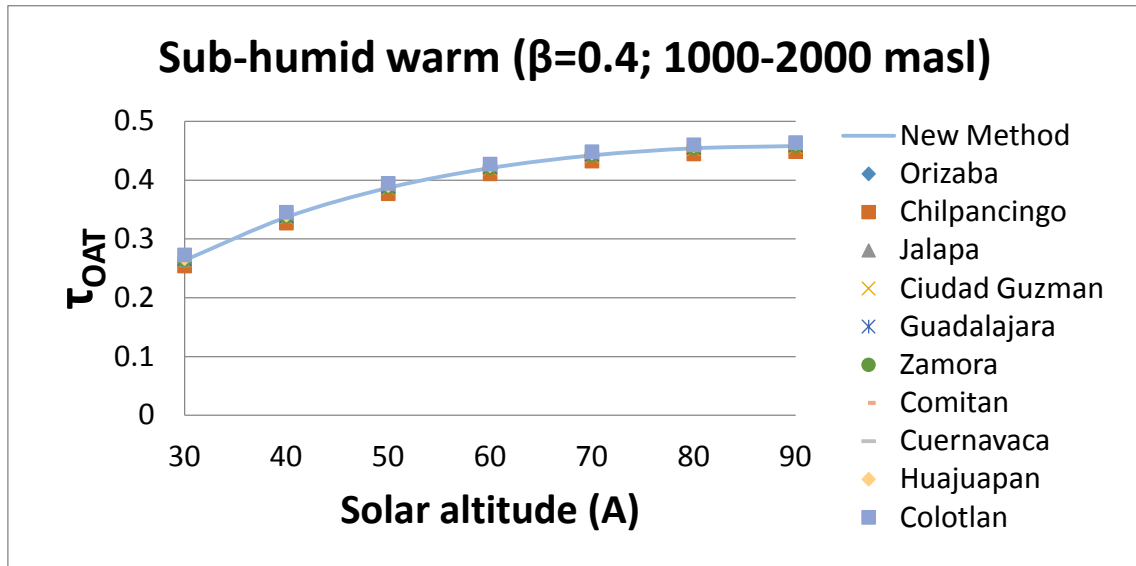


Figure 3. Overall atmospheric transmittance ( $\tau_{OAT}$ ) versus solar altitude (A) for the sub-humid warm climate, very turbid atmosphere ( $\beta=0.4$ ) and altitude interval 1000-2000 masl

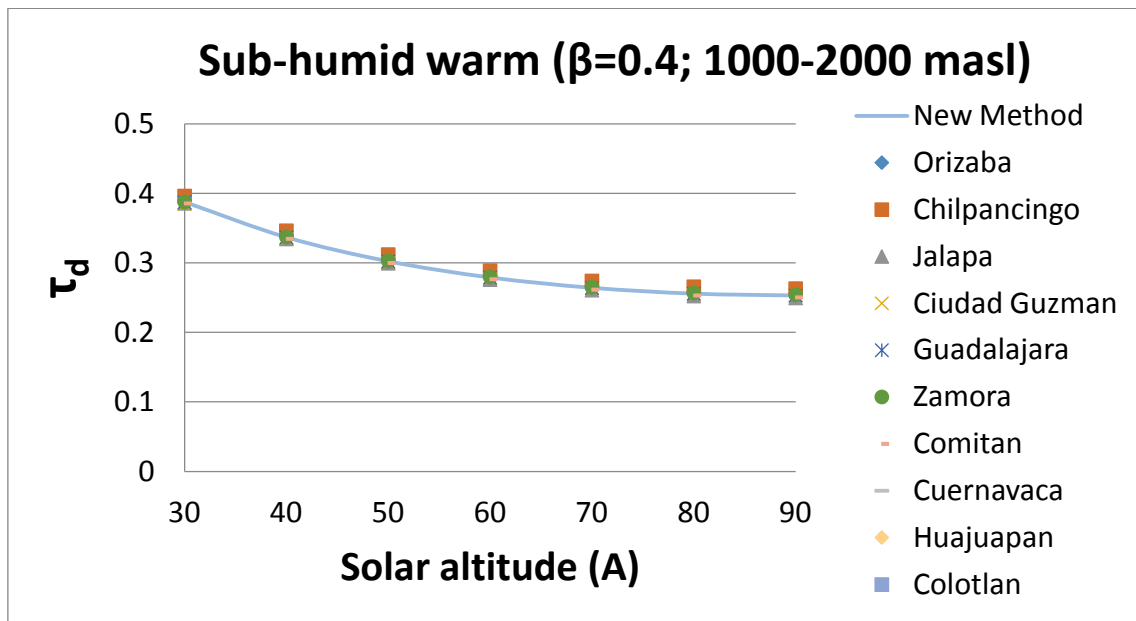


Figure 4. Diffuse global transmittance ( $\tau_{diff}$ ) versus solar altitude (A) for the sub-humid warm climate, very turbid atmosphere ( $\beta=0.4$ ) and altitude interval 1000-2000 masl

Table 3 shows the values and confident intervals of parameters  $a$  and  $b$  by climate, altitude and type of atmosphere with a confidence level of 0.95.

Table 3. Values and confident intervals of parameters  $a$  and  $b$  by climate, altitude and type of atmosphere in Mexico

Climate	$\beta$	0	0.1	0.2	0.3	0.4
Warm-humid	a (0-1000 masl)	0.822±0.0058	0.821±0.0056	0.809±0.0056	0.790±0.0055	0.771±0.0053
	b (0-1000 masl)	0.092±0.0012	0.250±0.0022	0.394±0.0037	0.509±0.0045	0.631±0.0058
Sub-humid warm	a (0-1000 masl)	0.821±0.0057	0.820±0.0056	0.811±0.0055	0.790±0.0055	0.763±0.0053
	b (0-1000 masl)	0.090±0.0008	0.239±0.0020	0.391±0.0030	0.512±0.0029	0.620±0.0024
	a (1000-2000 masl)	0.849±0.0059	0.843±0.0058	0.841±0.0058	0.823±0.0057	0.800±0.0056
	b (1000-2000 masl)	0.081±0.0007	0.220±0.0019	0.339±0.0030	0.449±0.0040	0.562±0.0051
Dry	a (0-1000 masl)	0.813±0.0065	0.812±0.0063	0.790±0.0063	0.782±0.0062	0.749±0.0050
	b (0-1000 masl)	0.072±0.0007	0.224±0.0019	0.348±0.0028	0.470±0.0039	0.582±0.0049
	a (1000-2000 masl)	0.831±0.0074	0.820±0.0071	0.819±0.0070	0.800±0.0070	0.783±0.0069
	b (1000-2000 masl)	0.076±0.0007	0.206±0.0020	0.323±0.0032	0.429±0.0043	0.530±0.0053
Very dry	a (0-1000 masl)	0.815±0.0081	0.806±0.0080	0.801±0.0080	0.779±0.0078	0.752±0.0075
	b (0-1000 masl)	0.082±0.0018	0.237±0.0031	0.376±0.0030	0.503±0.0035	0.606±0.0043
Sub-humid mild	a (1000-2000 masl)	0.833±0.0078	0.830±0.0077	0.819±0.0067	0.811±0.0063	0.789±0.0065
	b (1000-2000 masl)	0.071±0.0015	0.214±0.0023	0.333±0.0021	0.445±0.0022	0.542±0.0027
	a (> 2000 masl)	0.843±0.0077	0.842±0.0078	0.840±0.0062	0.827±0.0060	0.811±0.0081
	b (> 2000 masl)	0.073±0.0017	0.203±0.0021	0.314±0.0025	0.417±0.0032	0.516±0.0043

### 5.1.1 Warm-humid climate

Warm-humid climate is found in greater proportion in the coastal plain of the Gulf of Mexico, the Isthmus of Tehuantepec and the Sierra de los Tuxtlas. The altitude of these areas does not exceed 1000 masl. The values of parameters  $a$  and  $b$  obtained for the weather stations located in these areas are shown in Figure 5.

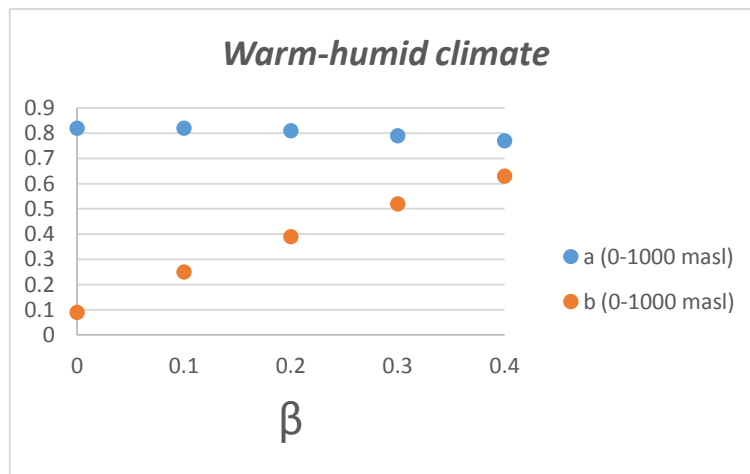


Figure 5. Parameters  $a$  and  $b$  versus degree of turbidity of the atmosphere ( $\beta$ ) for Warm-humid climate and altitudes lower than 1000 masl in Mexico

Parameter  $a$  is nearly constant (0.8) with the type of atmosphere, slightly decreasing when the turbidity increases; but parameter  $b$  ranges approximately from 0.1 to 0.6, increasing almost linearly with the degree of turbidity. Those results are coherent with the definition of  $a$  and  $b$  parameters. Parameter  $a$  is nearly constant, meaning that the energy per unit area when solar beams enter the atmosphere is similar

for the different types of atmosphere, and parameter  $b$  shows that the probability of a solar ray being intercepted at a point increases when the turbidity degree increases.

### 5.1.2 Sub-humid warm climate

Sub-humid warm climate has two classifications depending on the altitude, because this climate can be found in various parts of the country, from the north and center of the Coastal Plain of the Gulf of Mexico to the Isthmus of Tehuantepec, Plateau of Zohlaguna and the entire Yucatan Peninsula. In these places, altitudes are up to 1000 masl. This climate also corresponds to the Pacific zone, including the Central Depression of Chiapas, the Pacific Coastal Plain, the Sierra Madre del Sur and Sierra Pacific, where the altitude ranges between 1000 and 2000 masl.

Figure 6 shows the values of  $a$  and  $b$  parameters for Sub-humid warm climate taking into account the different altitudes. The trends are the same as those obtained for warm-humid climate and the higher the altitude (lower distance travelled by solar beams), the higher the  $a$  parameter (greater maximum flux density of solar radiation) but the lower the  $b$  parameter values (lower attenuation).

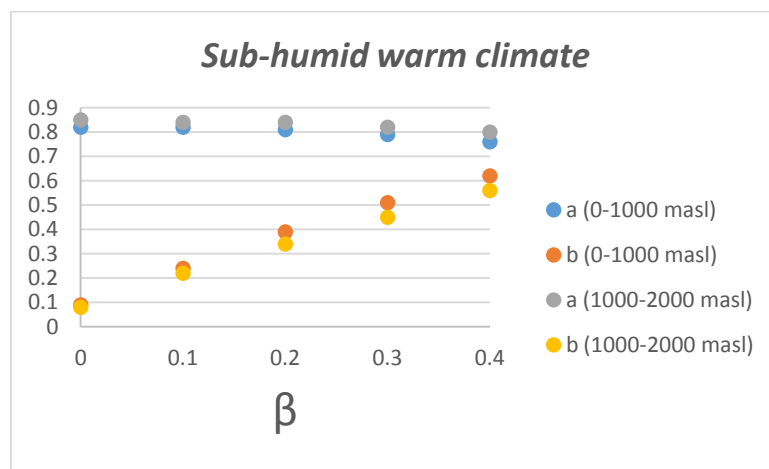


Figure 6. Parameters  $a$  and  $b$  versus degree of turbidity of the atmosphere ( $\beta$ ) for Sub-humid warm climate and different altitudes in Mexico

### 5.1.3 Dry climate

The dry climate, although in a small proportion, is present in the coastal area of Yucatan, the Blas basin and part of the Sierra Pacific. In these places the altitude does not exceed 1000 masl. This climate is also present on the Mexican Plateau, Northern Plateau, part of the Sierra Madre Oriental, the Sierra de Guanajuato, the Sierra de Zacatecas and part of the mountainous areas of Baja California, where the altitudes reach 2000 masl.

Figure 7 shows the values of parameters  $a$  and  $b$ , taking into account the different altitudes.

1  
2  
3  
4  
5  
6  
7  
8  
9  
10  
11  
12  
13  
14  
15  
16  
17  
18  
19  
20  
21  
22  
23  
24  
25  
26  
27  
28  
29  
30  
31  
32  
33  
34  
35  
36  
37  
38  
39  
40  
41  
42  
43  
44  
45  
46  
47  
48  
49  
50  
51  
52  
53  
54  
55  
56  
57  
58  
59  
60  
61  
62  
63  
64  
65

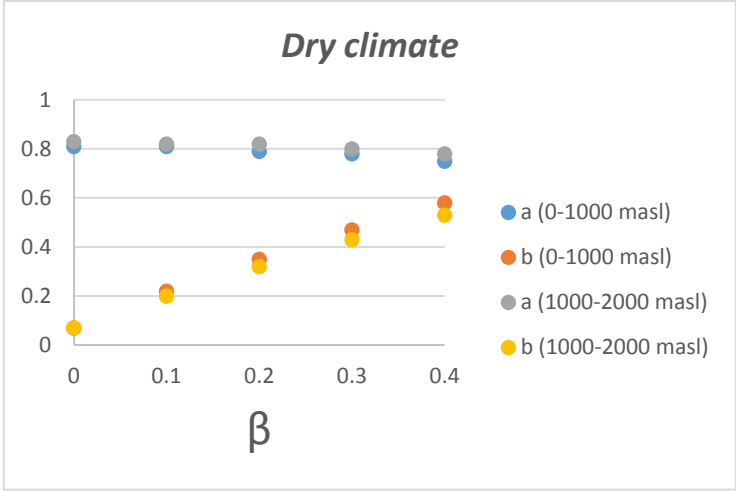


Figure 7. Parameters  $a$  and  $b$  versus degree of turbidity of the atmosphere ( $\beta$ ) for Dry climate and different altitudes in Mexico

5.1.4 Very dry climate

Climate Very dry is mainly located on the Peninsula of Baja California, the Pacific Coastal Plain and the Altar Desert, where altitudes are not higher than 1000 masl. Parameters  $a$  and  $b$  are shown in Figure 8.

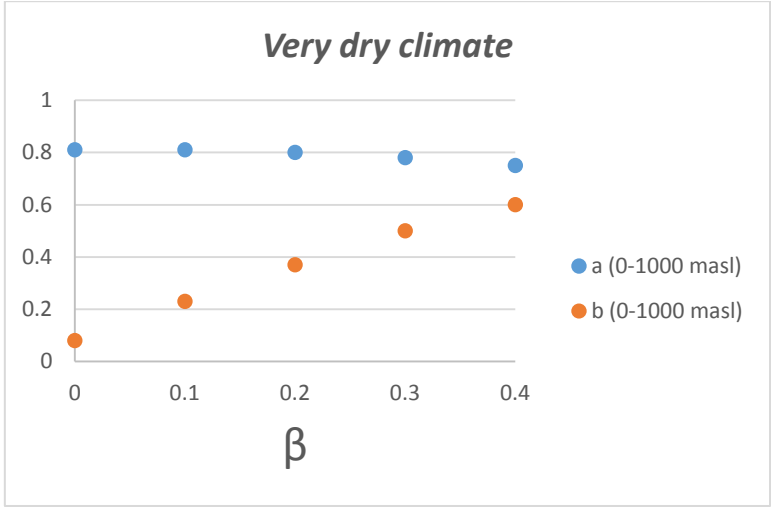


Figure 8. Parameters  $a$  and  $b$  versus degree of turbidity of the atmosphere ( $\beta$ ) for Very dry climate and altitudes lower than 1000 masl in Mexico

5.1.5 Sub-humid mild climate

Finally, the Sub-humid mild climate, is located towards the interior of the Country, in the foothills of the Sierra Madre Occidental and Oriental, the Sierra de Durango, the Sierra Madre del Sur, the Sierra de Miahuatlan and the region of the Mixteca, so registered altitudes range from 1000 masl to 2000 masl. This climate is also present in the higher regions of the Sierra Madre Occidental and the Sierra Madre del Sur, as well as the whole Transversal Volcanic System. In these areas the altitude exceeds 2000 masl. Figure 9 shows the values of parameters  $a$  and  $b$  for this climate.

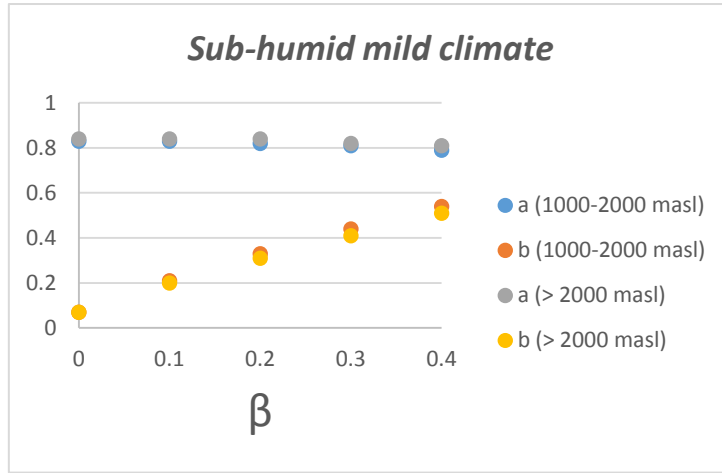


Figure 9. Parameters  $a$  and  $b$  versus degree of turbidity of the atmosphere ( $\beta$ ) for Sub-humid mild climate and different altitudes in Mexico

### 5.2 Diffuse Solar Irradiance Parameters

Similarly, the values of parameters  $B$  y  $B'$  for each type of climate and atmosphere were calculated. Results indicate that the values of these parameters are virtually identical for warm-humid and sub-humid warm climates, as well for dry and very dry climates, with differences lower than 2%. In addition, differences smaller than 1% in  $B$  and  $B'$  values were obtained for Clear, Slightly turbid, Turbid and Very turbid atmospheres. For this reason, the values of  $B$  and  $B'$  have been regrouped as shown in Table 4. This table also shows the confident intervals with a confidence level of 0.95.

Table 4. Values and confident intervals of parameters  $B$  and  $B'$  by climate, altitude and type of atmosphere in Mexico

Climate	$\beta$	0-1000 masl		1000-2000 masl		>2000 masl	
		0	0.1-0.4	0	0.1-0.4	0	0.1-0.4
Warm-humid & Sub-humid warm	B	0.261±0.0011	0.570±0.0061	0.272±0.0032	0.571±0.0056		
	B'	0.283±0.0033	0.689±0.0071	0.281±0.0019	0.668±0.0081		
Dry & Very dry	B	0.312±0.0081	0.569±0.0077	0.303±0.0063	0.567±0.0083		
	B'	0.343±0.0086	0.691±0.0081	0.322±0.0052	0.681±0.0080		
Sub-humid mild	B			0.299±0.0061	0.572±0.0079	0.283±0.0057	0.583±0.0072
	B'			0.319±0.0070	0.673±0.0064	0.303±0.0062	0.681±0.0081

### 5.3 Application and validation of the new method

As an example, the application of the new method is firstly used to determine the maximum direct solar irradiance that affects the weather station at Tapachula-Chiapas in February. The average maximum solar altitude ( $A$ ) is  $61^\circ$  and it is located in an area with predominantly sub-humid warm climate at 118 masl.

With these data and using the corresponding values of  $a$  and  $b$  from Figure 6, as well as Equations 39 and 34,  $\tau_{OAT}$  and  $I_{DH}$  were obtained respectively.

In Table 5 results are compared with those obtained using the Bird & Hulstrom method for the weather station located in Tapachula-Chiapas.

Table 5. Values of  $\tau_{OAT}$  and  $I_{DH}$  for Tapachula-Chiapas

$\beta$	0	0.1	0.2	0.3	0.4
$\tau_{OAT}$	0.74	0.62	0.52	0.44	0.37
$I_{DH}$ (W/m <sup>2</sup> ) using the new method	855	712	599	504	433
$I_{DH}$ (W/m <sup>2</sup> ) using Bird & Hulstrom method	868	724	609	515	440
<b>Error (%)</b>	1.5	1.8	1.6	2.2	1.6

Table 5 shows that the obtained values of direct solar irradiance are very similar for both the Bird & Hulstrom and the new method with error percentages lower than 2.5%.

The same comparison was done for all the weather stations finding similar error percentages. Therefore, the new method is proved to be a fast and accurate tool to obtain direct solar irradiance.

The advantage of the proposed alternative method is that direct solar irradiance can be calculated quite easily for five types of atmospheres, giving more information about available solar resources. Table 5 shows that the  $I_{HD}$  that affects Tapachula Chiapas in February may vary depending on the turbidity of the sky, so that it takes a value of 0.74 for a clean sky, and 0.37 for a very turbid sky. It means that the  $I_{HD}$  on a cloudy day can be reduced by up to 50%.

Diffuse solar irradiance has been calculated from Equations 40 and 41 taking into account the corresponding values of parameters  $B$  and  $B'$  from Table 4. The results obtained are compared with the Bird & Hulstrom method, and the values are shown in Table 6.

Table 6. Values of  $k_d$  and  $I_{dH}$  for Tapachula-Chiapas

$\beta$	0	0.1	0.2	0.3	0.4
$\tau_{diff}$	0.05	0.14	0.21	0.27	0.31
$I_{dH}$ (W/m <sup>2</sup> ) using the new method	63	173	254	322	372
$I_{dH}$ (W/m <sup>2</sup> ) using Bird & Hulstrom method	66	171	255	322	376
<b>Error (%)</b>	4.3	1.3	0.5	0.0	1.0

Table 6 shows that the  $I_{dD}$  in Tapachula Chiapas in February varies according to the type of atmosphere, so that on a cloudy day the diffuse solar irradiance can increase up to 5 times with respect to a clear sky.  $I_{dD}$  values obtained with the new method show a maximum variation from the Bird & Hulstrom method of 4.3%. This difference is acceptable to quantify the effects of solar radiation.

The total solar irradiance for this particular case is shown in Table 7. Differences with the Bird & Hulstrom method are lower than 2%.

Table 7. Values of  $I_{TH}$  for Tapachula-Chiapas

$\beta$	0	0.1	0.2	0.3	0.4
$I_{TH}$ (W/m <sup>2</sup> ) using the new method	918	885	853	825	805
$I_{TH}$ (W/m <sup>2</sup> ) using Bird & Hulstrom method	934	895	864	837	816
<b>Error (%)</b>	1.7	1.1	1.3	1.4	1.3

The same procedure was performed for the different climates and altitudes to obtain the direct, diffuse and total solar irradiance. The results were compared with those obtained with the Bird & Hulstrom model, finding differences between the two models lower than 5%. These results indicate that the new method to compute the availability of solar radiation in Mexico is accurate and very efficient, and that its application does not involve significant errors in the quantification of the solar resource.

The average solar resource ( $\text{kWh}/\text{m}^2\text{-day}$ ) was also calculated from the solar irradiances obtained with the new method for each type of atmosphere. These results were compared with the monthly average solar energy for some Mexican states, obtained by Hernández-Escobedo et al. [35] from experimental data.

Figures 10 to 13 show the monthly average solar resource obtained experimentally and by the new method at Veracruz, Tabasco, Campeche and Yucatán States. As it can be seen, the experimental values fit quite well between the range defined by the turbidity degree (extremely clean and very turbid).

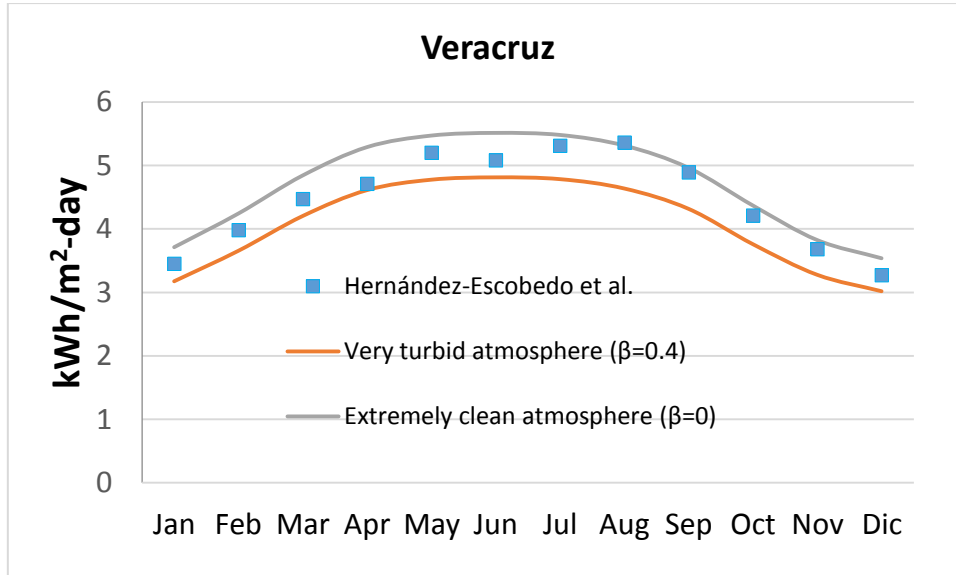


Figure 10. Comparison between the monthly average solar resource obtained by Escobedo et al. and the new method (extremely clean and very turbid atmosphere) at Veracruz State.

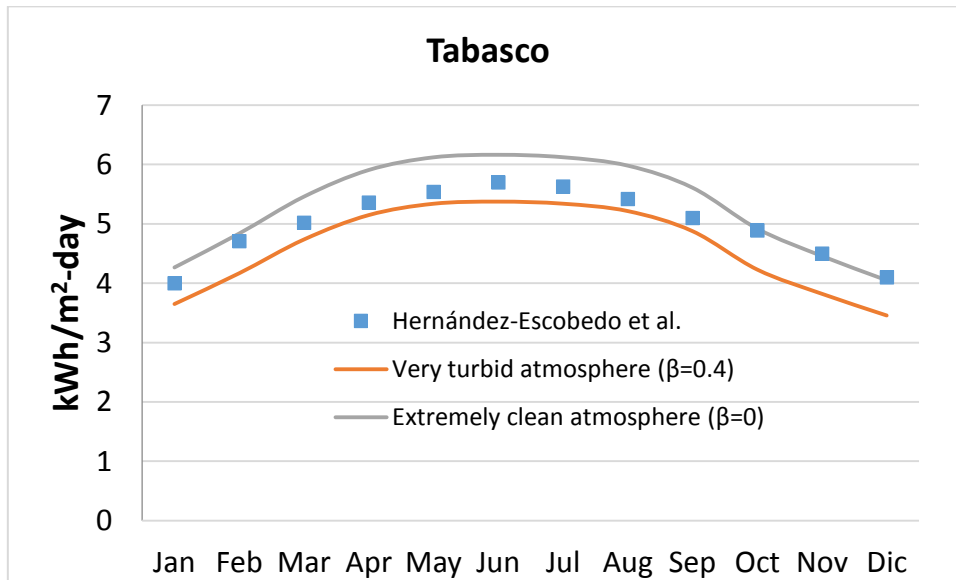


Figure 11. Comparison between the monthly average solar resource obtained by Escobedo et al. and the new method (extremely clean and very turbid atmosphere) at Tabasco State.

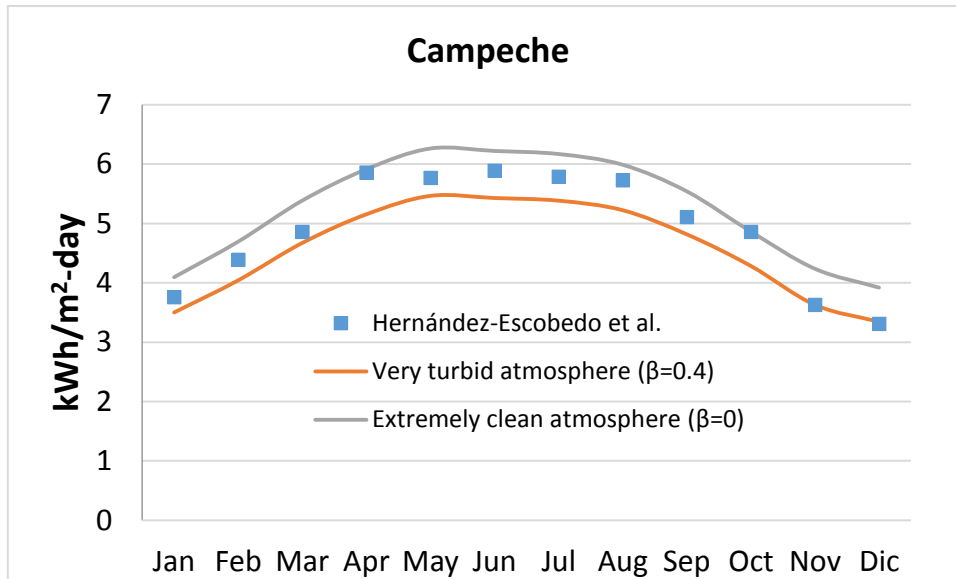


Figure 12. Comparison between the monthly average solar resource obtained by Escobedo et al. and the new method (extremely clean and very turbid atmosphere) at Campeche State.

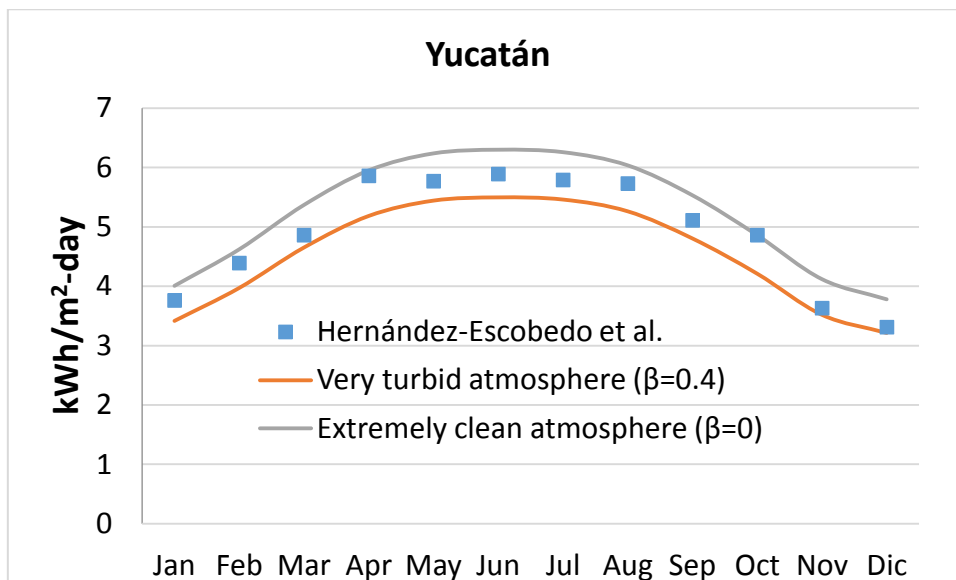


Figure 13. Comparison between the monthly average solar resource obtained by Escobedo et al. and the new method (extremely clean and very turbid atmosphere) at Yucatán State.

## 6. Conclusions

This paper analyzes the attenuation processes of the solar radiation taking into account the effects of meteorological and climate conditions. The state of the art in this field is presented, together with a review of the most significant analytical models for solar irradiance calculation. Specifically the Bird and Hulstrom model (the most complete and accurate) is explained in detail, including an overview of its different variations.

Following this revision, a new method based on the atmospheric transmittance is developed. It presents a clear advantage over the traditional Bird & Hulstrom model because it reduces the calculation process to obtain the solar irradiances. Only five simple equations are required depending on the type of climate, altitude and solar altitude instead of the more than fifteen complex equations depending on over ten variables of the Bird & Hulstrom model. This method also allows to quantify the influence of the turbidity degree in both direct and diffuse irradiances. That information is essential to select which solar technologies are suitable in each location.



1 As an application, the new method has been implemented and characterized in Mexico. Meteorological  
2 records of 20 years corresponding to 74 weather stations in Mexico have been used to determine the  
3 parameters required. The results obtained for the overall atmospheric transmittance showed that the type  
4 of climate is not the only variable that determines the attenuation; the geography of the site was found to  
5 be another important element for the quantification. Thus, to determine the definitive parameters  
6 employed by the new method, the five types of climates predominant in Mexico have been considered,  
7 together with three altitude ranges.

8 The results show variations smaller than 5% when compared to the Bird & Hulstrom model and they have  
9 been also validated with experimental data available for different locations. The characteristics of the new  
10 method make it a fast, simple and reliable procedure to estimate the solar irradiance, especially for those  
11 places where direct information is not available.

12 The numerical values of the parameters have been obtained specifically for Mexico, but it should be  
13 applicable elsewhere. Nonetheless, the grouping in climates and altitudes should be further tested, being  
14 the most sensitive aspect of the methodology.

## 15 **References**

---

16  
17  
18  
19  
20 [1] Prieto, J.I. Capitulo II. Disponibilidad de la Energía Solar. Universidad de Oviedo, Departamento de Máquinas y Motores  
21 Térmicos. Mayo 2008. Oviedo, España.

22 [2] Martínez, A.I. Tesis de Licenciatura, Sistemas fotovoltaicos conectados a red. Planta Fotovoltaica 20 MW Portusa.  
23 Departamento de Energía. Universidad de Oviedo, 2007. Oviedo, España.

24 [3] Medidor de partículas KM3887. Manual de equipos de medida para la industria, el comercio y la investigación (2011). Albacete.  
25 España.

26 [4] Du, H., Li, N., Brown, M. A., Peng, Y., & Shuai, Y. (2014). A bibliographic analysis of recent solar energy literatures: The  
27 expansion and evolution of a research field. *Renewable Energy*, 66, 696-706.

28 [5] Timilsina, Govinda R., Lado Kurdgelashvili, and Patrick A. Narbel. Solar energy: Markets, economics and policies. *Renewable  
29 and Sustainable Energy Reviews* 16.1 (2012): 449-465.

30 [6] Solangi, K. H., Islam, M. R., Saidur, R., Rahim, N. A., & Fayaz, H. (2011). A review on global solar energy policy. *Renewable  
31 and sustainable energy reviews*, 15(4), 2149-2163.

32 [7] Fariba B., Ali A., Ahmad R. Empirical models for estimating global solar radiation: A review and case study. *Renewable and  
33 Sustainable Energy Reviews*, 21, 798-821. 2013.

34 [8] Islam, M. D., Kubo, I., Ohadi, M., & Alili, A. A. (2009). Measurement of solar energy radiation in Abu Dhabi, UAE. *Applied  
35 Energy*, 86(4), 511-515.

36 [9] Islam, M. D., Alili, A. A., Kubo, I., & Ohadi, M. (2010). Measurement of solar-energy (direct beam radiation) in Abu Dhabi,  
37 UAE. *Renewable Energy*, 35(2), 515-519.

38 [10] Gherboudj, I., & Ghedira, H. (2015). Assessment of solar energy potential over the United Arab Emirates using remote sensing  
39 and weather forecast data. *Renewable and Sustainable Energy Reviews*.

40 [11] N. Vera. Tesis Doctoral. Atlas climático de irradiación solar a partir de imágenes del satélite NOAA. Aplicación a la Península  
41 Ibérica. Universidad Politécnica de Cataluña. Barcelona España, Mayo 2005.

42 [12] Yadav, A. K., & Chandel, S. S. (2015). Solar energy potential assessment of western Himalayan Indian state of Himachal  
43 Pradesh using J48 algorithm of WEKA in ANN based prediction model. *Renewable Energy*, 75, 675-693.

44 [13] Sorapipatana C. An. Assessment of solar Energy potential in Kampuchea. *Renewable & Sustainable Energy Reviews* 2010; 14:  
45 2174-8.

46 [14] Can Ertekin, Osman Yaldiz. Comparison of some existing models for estimating global solar radiation for Antalya (Turkey).  
47 *Energy Conversion & Management*. 41 (2000) 311±330. Junio 1999.

48 [15] Khatib, T., Mohamed, A., & Sopian, K. (2012). A review of solar energy modeling techniques. *Renewable and Sustainable  
49 Energy Reviews*, 16(5), 2864-2869.

50 [16] El Ouderni, A. R., Maatallah, T., El Alimi, S., & Nassrallah, S. B. (2013). Experimental assessment of the solar energy  
51 potential in the gulf of Tunis, Tunisia. *Renewable and Sustainable Energy Reviews*, 20, 155-168.

- 
- 1 [17] Comparative study of mathematical models in estimating solar irradiance for Australia  
2  
3 [18] Sözen, A., & Arcakliog̃lu, E. (2005). Effect of relative humidity on solar potential. *Applied energy*, 82(4), 345-367.  
4  
5 [19] Fadare, D. A. (2009). Modelling of solar energy potential in Nigeria using an artificial neural network model. *Applied Energy*,  
6 86(9), 1410-1422.  
7 [20] Sözen, A., Arcakliog̃lu, E., Özalp, M., & Kanit, E. G. (2004). Use of artificial neural networks for mapping of solar potential in  
8 Turkey. *Applied Energy*, 77(3), 273-286.  
9  
10 [21] Sözen, A., & Arcakliog̃lu, E. (2005). Solar potential in Turkey. *Applied Energy*, 80(1), 35-45.  
11  
12 [22] Sözen, A., Arcakliog̃lu, E., Özalp, M., & Kanit, E. G. (2005). Solar-energy potential in Turkey. *Applied Energy*, 80(4), 367-  
13 381.  
14 [23] Gutierrez-Corea, F. V., Manso-Callejo, M. A., Moreno-Regidor, M. P., & Manrique-Sancho, M. T. (2016). Forecasting short-  
15 term solar irradiance based on artificial neural networks and data from neighboring meteorological stations. *Solar Energy*, 134, 119-  
16 131.  
17 [24] Pan, T., Wu, S., Dai, E., & Liu, Y. (2013). Estimating the daily global solar radiation spatial distribution from diurnal  
18 temperature ranges over the Tibetan Plateau in China. *Applied Energy*, 107, 384-393.  
19  
20 [25] Bristow KL, Campbell GS. On the relationship between incoming solar radiation and daily maximum and minimum  
21 temperature. *Agric Forest Meteorol* 1984; 31(2):159-66.  
22 [26] Grindley, P. C., Batty, W. J., & Probert, S. D. (1995). Mathematical model for predicting the magnitudes of total, diffuse, and  
23 direct-beam insolation. *Applied energy*, 52(2), 89-110.  
24 [27] Liu, Y., Shimada, S., Yoshino, J., Kobayashi, T., Miwa, Y., & Furuta, K. (2016). Ensemble forecasting of solar irradiance by  
25 applying a mesoscale meteorological model. *Solar Energy*, 136, 597-605.  
26 [28] Kurtz, B., & Kleissl, J. (2017). Measuring diffuse, direct, and global irradiance using a sky imager. *Solar Energy*, 141, 311-322.  
27  
28 [29] Lou, S., Li, D. H., Lam, J. C., & Chan, W. W. (2016). Prediction of diffuse solar irradiance using machine learning and  
29 multivariable regression. *Applied Energy*, 181, 367-374.  
30  
31 [30] Chu, Y., & Coimbra, C. F. (2017). Short-term probabilistic forecasts for Direct Normal Irradiance. *Renewable Energy*, 101,  
32 526-536.  
33  
34 [31] Bird R. Hulstrom R. A simplified clear sky model for direct and diffuse insolation on horizontal surfaces. *Solar Energy*  
35 Research Institute, EEUU 1981.  
36 [32] Pinazo, J.M. Manual de Climatización, Tomo II. Universidad Politécnica de Valencia. ISBN 84-7721-341-0. 1995. España.  
37  
38 [33] Bosca J. V. Tesis Doctoral: Contribución al estudio de la radiación solar y de la determinación de la turbiedad atmosférica.  
39 Aplicaciones a Valencia y Sevilla. Universidad Politécnica de Valencia. 1995. Valencia, España.  
40  
41 [34] Villcaña-Ortiz, E., Gutiérrez-Trashorras, A. J., Paredes-Sánchez, J. P., & Xiberta-Bernat, J. (2015). Solar energy potential in  
42 the coastal zone of the Gulf of Mexico. *Renewable Energy*, 81, 534-542.  
43  
44 [35] Hernández-Escobedo, Q., Rodríguez-García, E., Saldaña-Flores, R., Fernández-García, A., & Manzano-Agugliaro, F. (2015).  
45 Solar energy resource assessment in Mexican states along the Gulf of Mexico. *Renewable and Sustainable Energy Reviews*, 43,  
46 216-238.  
47 [36] Rivas, D., Saleme-Vila, S., Ortega-Izaguirre, R., Chalé-Lara, F., & Caballero-Briones, F. (2013). A climatological estimate of  
48 incident solar energy in Tamaulipas, northeastern Mexico. *Renewable Energy*, 60, 293-301.  
49  
50 [37] Cancino S.Y, Gutiérrez-T.A., Xiberta-B.J Current state of wind energy in Mexico, achievements and perspectives Review  
51 Article. *Renewable and Sustainable Energy Reviews*, Volume 15, Issue 8, October 2011, Pages 3552-3555.  
52 [38] Estrada C. Almanza R., Irradiaciones global, directa y difusa, en superficies horizontales e inclinadas, así como irradiación  
53 directa normal en la República Mexicana. Serie Investigación y Desarrollo. Instituto de Ingeniería de la UNAM. ISBN 970-32-  
54 0196-2. Mayo 2005. México.  
55 [39] Mapa de recurso solar. Sistema de Información Geográfica para las Energías renovables en México (SIGER). Instituto de  
56 Investigaciones Eléctricas (IIE). <http://sag01.iie.org.mx/evaluarer/SIGER.html> (Last accessed April 2017).  
57 [40] Estrada C., Cabanillas R., Hinojosa F., Pérez B., Ochoa M., Manrincic Irene., Regalado L. Ponencia Innovación para un futuro  
58 más brillante. Laboratorio Nacional de Sistemas de Concentración Solar y Química Solar UNISON-UNAM. Programa de  
59 transferencia de Tecnología TxTec. Abril 2008. México.  
60  
61  
62  
63  
64  
65

- 
- 1 [41] Agredano J. Prospectiva de las Tecnología Solar Fotovoltaica para la Generación de Electricidad. División de Energías  
2 Alternas. Instituto de Investigaciones Eléctricas (IIE). Anexo 7. 2005. México.
- 3 [42] Polo, J., Gastón, M., Vindel, J. M., & Pagola, I. (2015). Spatial variability and clustering of global solar irradiation in Vietnam  
4 from sunshine duration measurements. *Renewable and Sustainable Energy Reviews*, 42, 1326-1334.
- 5 [43] Nijegorodov, N., & Luhanga, P. V. C. (1998). A new model to predict direct normal instantaneous solar radiation, based on  
6 laws of spectroscopy, kinetic theory and thermodynamics. *Renewable Energy*, 13(4), 523-530.
- 7 [44] Mohammadi, K., & Khorasanizadeh, H. (2015). A review of solar radiation on vertically mounted solar surfaces and proper  
8 azimuth angles in six Iranian major cities. *Renewable and Sustainable Energy Reviews*, 47, 504-518.
- 9 [45] Eltbaakh, Y. A., Ruslan, M. H., Alghoul, M. A., Othman, M. Y., Sopian, K., & Razykov, T. M. (2012). Solar attenuation by  
10 aerosols: An overview. *Renewable and Sustainable Energy Reviews*, 16(6), 4264-4276.
- 11 [46] Kudish, A. I., & Evseev, E. G. (2011). The analysis of solar UVB radiation as a function of solar global radiation, ozone layer  
12 thickness and aerosol optical density. *Renewable Energy*, 36(6), 1854-1860.
- 13 [47] M.H. Saffaripour, M.A. Mehrabian. Numerical methods applied to global solar radiation modeling – comparison with  
14 measured data. *International Journal of Numerical Methods for Heat & Fluid Flow*. Vol. 19 No. 6, 2009 pp. 777-789. May 2008.
- 15 [48] Psiloglou, B. E., Santamouris, M., & Asimakopoulos, D. N. (1995). On broadband Rayleigh scattering in the atmosphere for  
16 solar radiation modelling. *Renewable energy*, 6(4), 429-433.
- 17 [49] Psiloglou, B. E., Santamouris, M., & Asimakopoulos, D. N. (1995). Predicting the broadband transmittance of the uniformly  
18 mixed gases (CO<sub>2</sub>, CO, N<sub>2</sub>O, CH<sub>4</sub> and O<sub>2</sub>) in the atmosphere, for solar radiation models. *Renewable energy*, 6(1), 63-70.
- 19 [50] Kataoka, N., Yoshida, S., Ueno, S., & Minemoto, T. (2014). Evaluation of solar spectral irradiance distribution using an index  
20 from a limited range of the solar spectrum. *Current Applied Physics*, 14(5), 731-737.
- 21 [51] Nikitidou, E., Kazantzidis, A., & Salamalikis, V. (2014). The aerosol effect on direct normal irradiance in Europe under clear  
22 skies. *Renewable Energy*, 68, 475-484.
- 23 [52] Shaltout, M. M., Tadros, M. T. Y., & El-Metwally, M. (2000). Studying the extinction coefficient due to aerosol particles at  
24 different spectral bands in some regions at great Cairo. *Renewable energy*, 19(4), 597-615.
- 25 [53] T. Moreno, Aerosoles Atmosféricos: Problemas Ambientales. Temas ambientales. [www.aulados.net](http://www.aulados.net). (Last accessed April  
26 2017).
- 27 [54] Tapakis, R., & Charalambides, A. G. (2014). Enhanced values of global irradiance due to the presence of clouds in Eastern  
28 Mediterranean. *Renewable Energy*, 62, 459-467.
- 29 [55] Hussain, M., Khatun, S., & Rasul, M. G. (2000). Determination of atmospheric turbidity in Bangladesh. *Renewable energy*,  
30 20(3), 325-332.
- 31 [56] Eltbaakh, Y. A., Ruslan, M. H., Alghoul, M. A., Othman, M. Y., & Sopian, K. (2012). Issues concerning atmospheric turbidity  
32 indices. *Renewable and Sustainable Energy Reviews*, 16(8), 6285-6294.
- 33 [57] Toledano O. Carlos. Tesis Doctoral: Climatología de los aerosoles mediante la caracterización de propiedades ópticas y masas  
34 de aire en la estación “El Arenillo” de la red Aeronet. Universidad de Valladolid. España 2005.
- 35 [58] B. Kusienska. Ponencia: La Concentración de Aerosoles en la Atmósfera inhibe la lluvia en la Ciudad de México.  
36 Departamento de Física de Nubes. UNAM-México. Boletín UNAM-DGCS-515. Agosto 2009. México.
- 37 [59] Chaâbane, M., Masmoudi, M., & Medhioub, K. (2004). Determination of Linke turbidity factor from solar radiation  
38 measurement in northern Tunisia. *Renewable energy*, 29(13), 2065-2076.
- 39 [60] C. Raichijk. Estimación del Índice de Turbidez de Linke para distintas Localidades de Argentina. GERSolar, Instituto de  
40 Ecología y Desarrollo Sustentable (INEDES), Departamento de Ciencias Básicas. Argentina 2009.
- 41 [61] Moon P., Proposed standard solar-radiation curves for engineering use. *Journal of the Franklin Institute* 1940, 583-617.
- 42 [62] Fowle F., The transparency of aqueous vapor. *Astrophysical Journal* 1915, 394-411.
- 43 [63] Läubli A., Zur absorption der ultravioletten Strahlung in Ozon. *Zeitschrift Für Physik a Hadrons and Nuclei* 1929, 92-94.
- 44 [64] Reddy J., An empirical method for the estimation of total solar radiation. *Solar Energy* 1971, 289-290.
- 45 [65] IDEAM, Atlas de radiación solar de Colombia (2005). República de Colombia: Centro de Documentación e Información  
46 Científica Técnica.
- 47 [66] ASHRAE, Handbook of fundamentals. New York 1972.
- 48  
49  
50  
51  
52  
53  
54  
55  
56  
57  
58  
59  
60  
61  
62  
63  
64  
65

- 
- 1 [67] Threlkeld J., Direct solar radiation available on clear days. American Society of Heating, Refrigeration and Air Condition  
2 Engineers 1958.  
3
- 4 [68] Lacis A., Hansen J., A parametrization for the absorption in solar radiation in the Earth's Atmosphere. Journal of the  
5 atmospheric sciences 1973, 118-133.  
6
- 7 [69] Manabe S., Strickler R., Thermal equilibrium in the atmosphere with a convective adjustment. Journal of the atmospheric  
8 sciences 1964, 361-385.  
9
- 10 [70] Hottel H., A simple model for estimating the transmittance of direct solar radiation through clear atmospheres. Solar Energy  
11 1976, 129-134.  
12
- 13 [71] Passamai V., Determinación de radiación solar horaria para días claros mediante planilla de cálculo. Facultad de Ciencias  
14 Exactas, Universidad Nacional de Salta, Argentina 2000.  
15
- 16 [72] Davies J., Calculation of the solar radiation incident on a horizontal surface (1979). Canadian Atmospheric Environment  
17 Service. First Canadian Solar Radiation Data Workshop.  
18
- 19 [73] Hoyt D., A model for calculation of solar global insolation. Solar Energy 1978, 27-35.  
20
- 21 [74] Yamamoto G., Direct absorption of solar radiation by atmospheric water vapor, carbon dioxide and molecular oxygen. Journal  
22 of the atmospheric sciences 1962, 182-188.  
23
- 24 [75] Burch D., Total absorbance in carbon dioxide in the infrared. Applied Optics 1962, 759-765.  
25
- 26 [76] Angstrom A., Techniques of determining the turbidity of the atmosphere. The Eppley Foundation for Research. Tellus XIII,  
27 1961.  
28
- 29 [77] Angstrom A., The parameters of atmospheric turbidity. The Eppley Foundation for Research. Tellus XVI, 1964.  
30
- 31 [78] Atwater M., Ball J., A surface solar radiation model for cloudy atmosphere. Monthly weather review 1980, 879-888.  
32
- 33 [79] McDonald J., Direct absorption of solar radiation by atmospheric water vapor. Journal of Meteorology 1960, 319-328.  
34
- 35 [80] Watt O., On the nature and distribution of solar radiation (1975). Departamento de Energía de EEUU.  
36
- 37 [81] Valley S., Handbook of geophysics and space environments (1965). Air Force Cambridge Research Labs Hanscom.  
38
- 39 [82] Wong, L. T., & Chow, W. K. (2001). Solar radiation model. Applied Energy, 69(3), 191-224.  
40
- 41 [83] Toledano O. Carlos. Tesis Doctoral: Climatología de los aerosoles mediante la caracterización de propiedades ópticas y masas  
42 de aire en la estación "El Arenillo" de la red Aeronet. Universidad de Valladolid. España 2005.  
43
- 44 [84] Mächler, M. Tesis de maestría: Parametrization of solar irradiation under clear skies. Departamento de Ingeniería Mecánica,  
45 Universidad de Columbia. Vancouver, Canadá. 1983.  
46
- 47 [85] Mächler, M. Tesis de maestría: Parametrization of solar irradiation under clear skies. Departamento de Ingeniería Mecánica,  
48 Universidad de Columbia. Vancouver, Canadá. 1983.  
49
- 50 [86] SMN, Sistema Meteorológico Nacional, Red de observatorios meteorológicos (1981-2010). Normales climatológicas,  
51 <http://smn.cna.gob.mx/esmas>. Acceso a la información en 2010-2011.  
52
- 53 [87] INEGI. Instituto Nacional de Estadística y Geografía. Mapoteca Digital Versión 2.0. <http://www.inegi.org.mx> .  
54
- 55 [88] Jáuregui E., Algunas alteraciones de largo periodo del clima de la Ciudad de México debidas a la urbanización. Departamento  
56 de Meteorología General, Centro de Ciencias de la Atmósfera, UNAM. México 1995.  
57
- 58 [89] Gueymard C., Critical analysis and performance assessment of clear sky solar irradiance models using theoretical and measured  
59 data. Solar Energy 1993, 121-138.  
60
- 61 [90] Wright J., Correlaciones de la fracción difusa. Tópicos Meteorológicos y Oceanográficos 2000, 15-18.  
62
- 63 [91] Collares M., Rabl. The average distribution of solar radiation—correlation between diffuse and hemispherical and daily and  
64 hourly insolation values. Solar Energy 1979, 155-164.  
65
- 66 [92] Orgill J., Hollands G., Correlation equation for hourly diffuse radiation on horizontal surface. Solar Energy 1977, 357-359.  
67
- 68 [93] Erbs G. et al, Klein S., Duffie J., Estimation of the diffuse radiation fraction for hourly, daily and monthly average global  
69 radiation. Solar Energy 1982, 293-304.  
70
- 71 [94] Spencer J., A comparison of methods for estimating hourly diffuse solar radiation from global solar radiation. Solar Energy  
72 1982, 19-32.

---

1 [95] Garcia G., Velarde J., Energías Renovables y Medio Ambiente. Centro de Estudios de Ordenación del Territorio y Medio  
2 Ambiente. España, 1982.

3 [96] Tung, C. P., Yang, Y. C. E., Lee, T. Y., & Li, M. H. (2007). Modification of a stream temperature model with Beer's law and  
4 application to GaoShan Creek in Taiwan. Ecological modelling, 200(1), 217-224.

5 [97] Forero N., Caicedo L., Gordillo G., Correlation of global solar radiation values estimated and measured on an inclined surface  
6 for clear days in Bogotá. Renewable Energy 2007, 2590-2602.

7  
8 [98] Mapa Hipsográfico y Batimétrico de México. Instituto de Geografía, Universidad Autónoma de México. INEGI. México Junio  
9 1989.

10  
11  
12  
13  
14  
15  
16  
17  
18  
19  
20  
21  
22  
23  
24  
25  
26  
27  
28  
29  
30  
31  
32  
33  
34  
35  
36  
37  
38  
39  
40  
41  
42  
43  
44  
45  
46  
47  
48  
49  
50  
51  
52  
53  
54  
55  
56  
57  
58  
59  
60  
61  
62  
63  
64  
65